Frequency specificity in intercellular communication

Influence of patterns of periodic signaling on target cell responsiveness

Yue-Xian Li and Albert Goldbeter
Faculté des Sciences, Université Libre de Bruxelles, B-1050 Brussels, Belgium

ABSTRACT Cells often communicate by means of periodic signals, as exemplified by a large number of hormones and by the aggregation of *Dictyostelium discoideum* amebas in response to periodic pulses of cyclic AMP. Periodic signaling allows bypassing the phenomenon of desensitization brought about by constant stimuli. To gain further insight into the efficiency of pulsatile signaling, we analyze the effect of periodic stimulation on the dynamic behavior of a receptor system capable of desensitization toward its ligand. We first show that the receptor system adapts to square-wave stimuli, i.e., the response eventually reaches a steady, periodic pattern after a transient phase. By analyzing the dependence of the response on the characteristics of the square-wave stimulation, we show that there exist a waveform and a period of that signal that result in maximum responsiveness of the target system. Similar results are obtained when the signal takes the more realistic form of a periodically repeated stimulation followed by exponential decay of the ligand. The results are discussed with respect to the role of pulsatile secretion of gonadotropin-releasing hormone (GnRH) by the hypothalamus and of periodic signaling by cyclic AMP pulses in *Dictyostelium*. The analysis accounts for the existence, in both cases, of an optimal frequency and waveform of the periodic stimulus that correspond to maximum target cell responsiveness.

INTRODUCTION

The regulation of cellular functions is largely accomplished through intercellular signaling. Thus, the binding of a hormone, neurotransmitter, or other ligand to receptors on target cells is an interaction of fundamental importance. A conspicuous property of this kind of interaction is its specificity. As pointed out by Weiss (1947) and also emphasized by Monod (1947), in spite of the widely different connotations of the word, any kind of specificity must, of necessity, be associated with a particular, "specific" pattern in space or time, or both. However, the understanding of the physical basis of specificity has so far mainly been restricted to the exploration of the molecular configurations, i.e., of spatial patterns only. Recent experimental results have revealed that beside this ligand specificity, the specific temporal pattern of stimulation is also of primary importance in many signal transduction systems where the conformational mutual fit of ligand with receptor alone cannot totally account for the observed specificity. This is particularly striking in the case of pulsatile hormone secretion, as exemplified by gonadotropin-releasing hormone (GnRH)-stimulated gonadotropin release. A pulsatile GnRH stimulus characterized by quite specific frequency, amplitude, and waveform is indeed required for normal reproductive activity in mammals (Belchetz et al., 1978; Knobil, 1980; Wildt et al., 1981; Pohl et al., 1983).

This temporal specificity of the stimulation pattern adds a new dimension, as pointed out by Knobil (1981), to our understanding of intercellular communication. As a matter of fact, the central nervous system controls fertility through alterations in the frequency of GnRH secretion (Karsch, 1987). Furthermore, a group of reproductive failures are classified according to the frequency or amplitude deviations of "wrong" signals from the adequate one (Wagner, 1985; Santoro et al., 1986). The list of systems exhibiting this kind of temporal specificity is rapidly growing, ranging from cyclic AMP (cAMP) signaling in the cellular slime mold *Dictyostelium discoideum* (Wurster, 1982; Goldbeter, 1987; Martiel and Goldbeter, 1987) to pulsatile patterns of hormone secretion observed for GnRH (Knobil, 1980), insulin or glucagon (Matthews et al., 1983; Verdin et al., 1984; Komjati et al., 1986), human pancreatic growth hormone-releasing factor (hpGRF) (Borges et al., 1984; Bassett and Gluckman, 1986), human corticotropin-releasing hormone (hCRH) (Avgerinos et al., 1986), arginine vasopressin (AVP) (Weitzman et al., 1977; Katz et al., 1979; Redekopp et al., 1986), thyrotropin (TSH) (Brabant et al., 1987), and arginine vasotocin (AVT) (Eggena, 1987). Modulation of intercellular communication by changes in temporally organized signals also

Y. X. Li is on leave from the Institute of Biophysics, Beijing, China.
Address correspondence and reprint requests to Dr. Goldbeter, Service de Chimie Physique, Université Libre de Bruxelles, Campus Plaine, C.P. 231, B-1050 Brussels, Belgium.

0006-3495/89/01/125/21 $2.00

occurs in the nervous system, where part of the information is carried by the pattern of electrical spikes (see Cazalis et al., 1985, for an example related to neuropeptide release).

The purpose of this paper is to investigate the physical mechanisms responsible for temporal specificity in intercellular communication. We shall focus our analysis on pulsatile patterns of hormone secretion and on pulsatile cAMP signaling in *Dictyostelium,* and will determine possible molecular bases of temporal specificity in these systems. Our goal is to demonstrate how the waveform and frequency of pulsatile signaling influence cellular responsiveness. A thorough understanding of this dynamic aspect of ligand–receptor interactions is clearly required for reaching a comprehensive view of signal transduction processes.

To determine the influence of the temporal pattern of stimulation on the cellular response, we shall use a model of a receptor system whose activity is triggered upon binding of a ligand. Prolonged incubation with the ligand induces desensitization, owing to the ligand-induced transition of the receptor into a less active state. A mathematical model of this kind has been developed through a series of experimental and theoretical studies initially devoted to bacterial chemotaxis (Macnab and Koshland, 1972; Koshland, 1977; Goldbeter and Koshland, 1982) and further analyzed in the context of exact sensory adaptation to constant stimuli (Segel et al., 1986; Knox et al., 1986).

Adaptation to continuous stimulation, which makes the system sensitive only to changes in ligand concentration, is closely associated with the phenomenon of temporal specificity. Both adaptation and the effect of various patterns of signaling can be studied in the same theoretical framework, as a function of the kinetic parameters governing receptor desensitization and resensitization. After presenting the model in Section 1, we obtain in Section 2 the response (expressed below in terms of some activity generated by the receptor system) to periodic stimuli which take the simple form of square-wave pulses. We then show that adaptation which occurs after a step increase in ligand (Segel et al., 1986) also occurs in the case of repetitive, pulsatile signaling: it takes then a characteristic time for the system to reach a steady pulsatile response. In Section 3, we demonstrate that the system exhibits temporal specificity toward signal frequency and waveform, that is, there exist an optimum frequency and an optimum waveform of the signal that result in maximum cellular responsiveness.

More realistic stimuli taking into account an exponential decrease of the ligand are considered in Section 4. We show by numerical simulations that an optimal pattern of stimulation also exists in these conditions, as in the case of square-wave stimuli.

An important conclusion of the analysis is that pulsatile patterns of intercellular communication are more efficient than continuous stimulation in systems which adapt to constant stimuli. Not all periodic patterns of stimulation, however, are equivalent as there exists a unique pattern that maximizes cellular responsiveness. In Section 5, we discuss how the results apply to the release of gonadotropins by the pituitary in response to pulses of GnRH delivered by the hypothalamus at a specific frequency. We also show how the analysis accounts for the existence of an optimal frequency of stimulation by cAMP pulses in *Dictyostelium* cells.

1. Model and kinetic equations

The model considered (Fig. 1) is that proposed by Segel et al. (1986) in the study of exact sensory adaptation. In this model, two receptor conformational states can transform into each other either through covalent modification or through simple conformational change. In either case, these correspond to nondesensitized (R) and desensitized (D) receptor states which differ by their capability of eliciting a cellular response upon binding of the ligand. Both receptor states combine with the ligand L to form the complexes $RL(\equiv X)$ and $DL(\equiv Y)$, thus creating a distribution among the four receptor species, while the

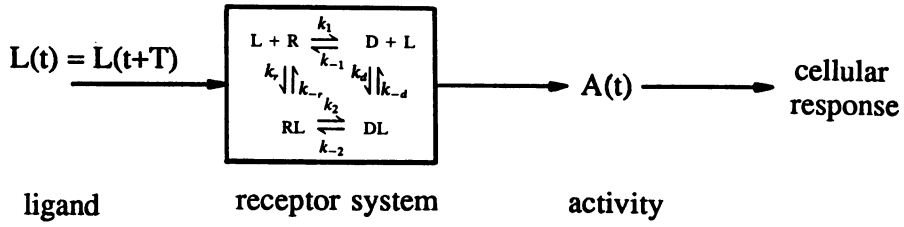

FIGURE 1. Schematic diagram of the receptor "box" subjected to the pulsatile ligand stimulus $L(t)$, that produces the periodic activity $A(t)$ associated with some cellular response. The interconversion between the two free receptor forms R and D, and the two liganded forms RL and DL are shown; the forms D and DL represent the desensitized state of the receptor. The kinetic coefficients for the receptor desensitization and for the ligand binding steps are indicated as well as the activity coefficients $a_i (i = 1, 2, 3, 4)$ that weight the contributions of the four receptor states to the activity.

total concentration of receptor R_T (=[R] + [X] + [Y] + [D]) remains fixed.

Binding of the ligand elicits the cellular response. The nature of this response as well as the precise manner by which it is linked to ligand binding differ from one particular system to another. In order to retain a character of generality to the present analysis, we do not specify at this stage either the nature of the response, or its relation to receptor saturation. Therefore, following Segel et al. (1986), we assume that the effect induced by the stimulus is measured by a quantity called activity,

$$A = a_1[R] + a_2[X] + a_3[Y] + a_4[D], \tag{1}$$

which is defined by Eq. 1 as a weighted linear combination of the concentrations of the four receptor states. The weight coefficient $a_i (i = 1, 2, 3, 4)$ represents the corresponding contribution of each receptor state to the ligand-induced cellular activity. Examples of how the activity may be related to the actual cellular response are discussed by Segel et al. (1986) as well as in Section 5 below.

The differential equation governing the time evolution of this system is (see also Segel et al., 1986):

$$\frac{d\mathbf{C}}{dt} = \mathbf{K}(L)\mathbf{C}, \tag{2}$$

where

$$\mathbf{C} = \begin{bmatrix} r \\ x \\ y \\ d \end{bmatrix},$$

$$\mathbf{K}(L) = \begin{bmatrix} -k_1 - k_r L & k_{-r} & 0 & k_{-1} \\ k_r L & -k_2 - k_{-r} & k_{-2} & 0 \\ 0 & k_2 & -k_{-2} - k_{-d} & k_d L \\ k_1 & 0 & k_{-d} & -k_{-1} - k_d L \end{bmatrix};$$

and $r \equiv [R]/R_T$, $x \equiv [RL]/R_T$, $y \equiv [DL]/R_T$, and $d \equiv [D]/R_T$ are the concentrations of the four receptor states scaled by the total concentration of the receptor, R_T. Now the conservation condition for the receptor and the definition of the scaled activity $\alpha = A/R_T$ become

$$r + x + y + d = 1; \tag{3}$$

$$\alpha(L) \equiv a_1 r + a_2 x + a_3 y + a_4 d. \tag{4}$$

The model was proposed to account for the biphasic response that follows a step increase in stimulus in many sensory systems. In the absence of ligand, the contribution of the R state of the receptor predominates over the contribution of the less active D state (i.e., $a_1 > a_4$). Upon increasing the level of ligand, the X state is formed, which possesses the highest activity coefficient a_2; this produces a "rapid" (compared with the slow receptor modification) increase in the activity level. The subsequent modification of X into Y, which state possesses a lower activity coefficient ($a_3 \ll a_2$) results in a progressive drop in the activity A. When conditions for exact adaptation are met (see Appendix and Segel et al., 1986), the activity at steady state returns to the prestimulus, basal value $A_0 = a_1 R + a_4 D$ regardless of the stimulus magnitude.

When the ligand is applied periodically, system (2) remains linear but with time-periodic coefficients, and subjected to the constraint (3). The solution of system (2) for the periodic stimulus $L(t) = L(t + T)$ should also be periodic with the same period T and should have the following form according to Floquet theory (Cesari, 1971):

$$\mathbf{C}(t) = \exp(\mathbf{\Lambda} t)\,\mathbf{S}(t)\,\mathbf{C}(0), \tag{5}$$

where $\mathbf{S}(t) = \mathbf{S}(t + T)$ with $\mathbf{S}(0) = \mathbf{I}$, and $\mathbf{\Lambda}$ is some time-independent matrix. For system (2) subjected to the constraint (3), the term $\exp(\mathbf{\Lambda} t)$, which eventually decreases to unity, governs the decrease in the amplitude of $\mathbf{C}(t)$. Two kinds of processes thus occur concomitantly: the adaptation described by the term $\exp(\mathbf{\Lambda} t)$, and the steady periodic response represented by the term $\mathbf{S}(t)$.

2. Response and adaptation to periodic, square-wave stimuli

In the present study, we first consider the square-wave signal (see Fig. 2):

$$\begin{aligned} \gamma(t) &= \gamma_1 \quad \text{if} \quad nT \le t < nT + \tau_1 \\ \gamma(t) &= \gamma_0 \quad \text{if} \quad nT + \tau_1 \le t \\ &\qquad < nT + \tau_1 + \tau_0 = (n+1)T, \end{aligned} \tag{6}$$

where $\tau_1 + \tau_0 = T$, and γ_j's ($\equiv L_j/K_R$, $K_R \equiv k_{-r}/k_r$, $j = 0, 1$) are the scaled ligand levels during the on-phase ($j = 1$) and off-phase ($j = 0$, $\gamma_1 > \gamma_0$) whose durations are denoted by τ_1 and τ_0, respectively, and $n = 1, 2, 3, \ldots$ represent the successive pulses in the repetitive stimulation. From now on, the subscripts 1 and 0 will always relate to the on-phase and the off-phase of the stimulus, respectively. We assume that $\gamma = 0$ before the onset of the signal.

Analytical solution for transient and asymptotic behavior

The detailed behavior of the activity α in response to this signal crucially depends on the time scale structure of the responding system. Two intrinsic time scales can be distinguished: the time that characterizes ligand binding, and the time associated with receptor desensitization. If the former exceeds the latter, no significant response could be observed because the system would always be in

an adapted state and therefore, would be unable to detect abrupt changes in ligand concentration. Accordingly, binding is usually much faster than adaptation. Under such conditions, it is a good approximation to assume that ligand binding is instantaneous compared with receptor modification or conformational change. Under this simplifying assumption to be retained in the present paper, the system becomes one dimensional (Segel et al., 1986). The time evolution of the four receptor states can be expressed as a function of the evolution of either the amount of receptor in active state, $R \equiv r + x$, or the amount of receptor in the inactive state, $D \equiv d + y = 1 - R$. Focusing on D (or R) is justified by the fact that these are the only quantities that behave continuously when the stimulus switches between the on- and the off-phases; all receptor concentrations can be obtained as a function of D (or R) (see Appendix, and Segel et al., 1986).

In the case of square-wave stimulation (Eq. 6 and Fig. 2) we obtain the following solution for the total fraction of desensitized receptor $D(t)$ and the activity $\alpha(t)$ in each of the successive phases of the periodic signal (see Appendix):

$$D_j^n(t) = D_s(\gamma_j) + [O_{1-j}^{n-j} - D_s(\gamma_j)] \exp\left(-\frac{t_j^n}{\tau_a(\gamma_j)}\right); \quad (7a)$$

$$\alpha_j^n(t) = \alpha_s(\gamma_j) - P(\gamma_j)\,[O_{1-j}^{n-j} - D_s(\gamma_j)] \exp\left(-\frac{t_j^n}{\tau_a(\gamma_j)}\right), \quad (7b)$$

where $t_j^n = t - (n-1)T - (1-j)\tau_1$ is the time in the jth phase of the nth period; by this definition time t_j^n is reset to zero at the beginning of each phase of the signal.

In the above equations, $n = 1, 2, 3, \ldots$ denote the successive pulses in the repetitive response, and the subscript j represents the on ($j = 1$) and off ($j = 0$) phases

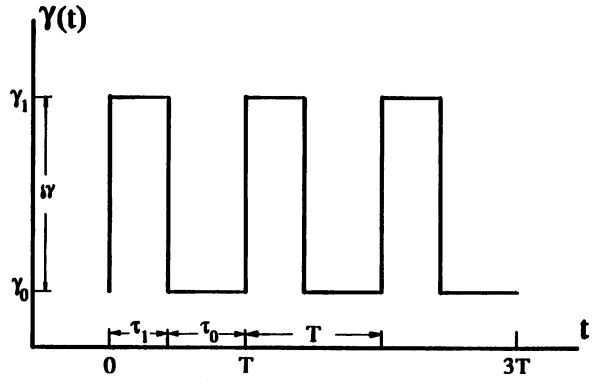

FIGURE 2. Square-wave periodic signal defined by Eq. 6. τ_1 and τ_0 represent, respectively, the duration of each stimulation (on-phase) and the time interval between stimulations (off-phase). γ_1 is the ligand level during the on-phase; γ_0 is the background ligand concentration during the off-phase. The period of the stimulus is $T = \tau_1 + \tau_0$.

within one signal period. O_1^n denotes the value of D at the end of the nth on-phase and the beginning of the nth off-phase, while O_0^n denotes the D value at the end of the nth off-phase and the beginning of the $(n+1)$th on-phase; the detailed forms of these functions are given in the Appendix. Appearing in Eqs. 7, a and b, are the functions:

$$D_s(\gamma) = u(\gamma)(u(\gamma) + v(\gamma))^{-1} \quad (8)$$

$$\alpha_s(\gamma) = R_s(\gamma)a(\gamma) + D_s(\gamma)b(\gamma) \quad (9)$$

$$P(\gamma) = a(\gamma) - b(\gamma) \quad (10)$$

$$\tau_a(\gamma) = (u(\gamma) + v(\gamma))^{-1} \quad (11)$$

with

$$u(\gamma) \equiv \frac{k_1 + k_2\gamma}{1 + \gamma} \quad (12a)$$

$$v(\gamma) \equiv \frac{k_{-1} + k_{-2}\gamma c}{1 + \gamma c} \quad (12b)$$

$$a(\gamma) \equiv \frac{a_1 + a_2\gamma}{1 + \gamma} \quad (13a)$$

$$b(\gamma) \equiv \frac{a_4 + a_3\gamma c}{1 + \gamma c}, \quad (13b)$$

where $c \equiv K_R/K_D$, $K_D \equiv k_{-d}/k_d$; $D_s(\gamma)$, $\alpha_s(\gamma)$ are the steady-state values of D and α after adaptation to a constant stimulus γ. In the case of exact adaptation (see Eq. A.5 in the Appendix, and Segel et al., 1986), the activity always returns to the same value at steady state, regardless of the level of the constant stimulus: $\alpha_s(\gamma_j) = \alpha_s(\gamma = 0) = \alpha_0$ ($j = 0, 1$) where $\alpha_0 = A_0/R_T$ is the normalized basal activity of the system in the absence of ligand L. In such a situation, the asymptotic activity is the same for both phases of the pulsatile stimulus. In the absence of exact adaptation, $\alpha_s(\gamma_0) \neq \alpha_s(\gamma_1) \neq \alpha_0$.

The quantity $\tau_a(\gamma)$ given by Eq. 11 is the adaptation time for the constant stimulus γ; it contains the contribution $u(\gamma)$ of receptor desensitization as well as the contribution $v(\gamma)$ of the reverse process of receptor resensitization. Finally, $P(\gamma)$ (Eq. 10) can be viewed (see Eq. 9) as the difference between the apparent weights $a(\gamma)$ and $b(\gamma)$ associated with the contributions of active and desensitized receptor states to the activity.

Adaptation to periodic stimuli

Shown in Fig. 3 are a typical time course of the activity of the receptor system triggered by a periodic square-wave stimulus, as well as the accompanying change in the fraction of desensitized receptor, D. A process of adaptation (dotted curves in Fig. 3) begins at the onset of the pulsatile signal. The system eventually reaches a steady,

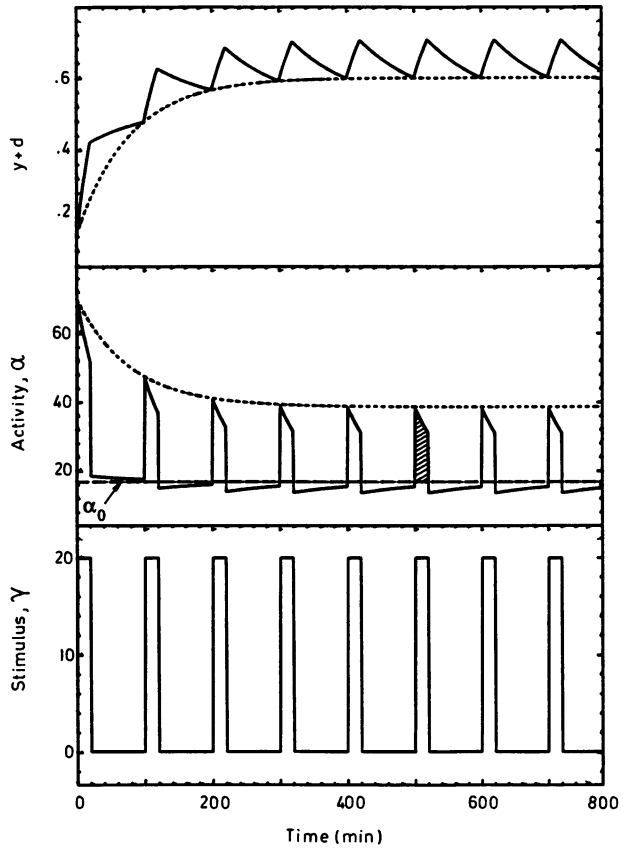

FIGURE 3. A typical activity curve (*middle panel*) generated by a periodic square-wave stimulus (*lower panel*) is shown, together with the time evolution of the fraction of desensitized receptor $(Y + D)/R_T$ (*top panel*). The parameters are: $a_1 = 20, a_4 = 1, a_3 = 10, a_2 = 85.1667$ (units of the activity coefficients are not specified as they depend on the nature of the cellular response triggered by the activity; see discussion); $k_1 = 0.004\ \text{min}^{-1}$, $k_{-1} = 0.02\ \text{min}^{-1}$, $k_2 = 0.02\ \text{min}^{-1}$, $k_{-2} = 0.002\ \text{min}^{-1}$; $k_r = 1\ \mu\text{M}^{-1}\text{min}^{-1}$, $k_{-r} = 25\ \text{min}^{-1}$, $k_d = 2\ \mu\text{M}^{-1}\text{min}^{-1}$, $k_{-d} = 1\ \text{min}^{-1}$; $\gamma_0 = 0.1$, $\gamma_1 = 20$, $\tau_1 = 20$ min, $\tau_0 = 80$ min; the system is subjected to the conditions for exact adaptation (A.5a, b) with $c = K_1/K_2 = 50$. The shaded area is defined as the integrated activity α_T.

periodic response generally characterized by a reduced amplitude.

The study of the long-term influence of the pulsatile stimulus on the response is meaningful only after the transient phase is completed and the steady response pattern is obtained. Before characterizing the asymptotic response, we shall first analyse the transient process. The time scale τ_p characterizing the adaptation to periodic stimuli is (see Eq. A.15, a and b, in Appendix):

$$\tau_p = \frac{T}{\omega_0 + \omega_1} = \frac{1+\beta}{\tau_a^{-1}(\gamma_0) + \tau_a^{-1}(\gamma_1)\beta} = \frac{1+\beta}{u(\gamma_0) + v(\gamma_0) + (u(\gamma_1) + v(\gamma_1))\beta}, \quad (14)$$

where $T(=\tau_0 + \tau_1)$ is the signal period; $\omega_j \equiv \tau_j/\tau_a\ (\gamma_j)$ $(j = 0, 1)$, $\beta \equiv \tau_1/\tau_0$ is the ratio between the durations of the on- and off-phases; $\tau_a(\gamma_j)(j = 0, 1)$, defined by Eq. 11, is the adaptation time of the system in response to the constant stimulus $\gamma = \gamma_j$.

What is surprising is that besides the amplitude of the signal, only the waveform of the stimulus characterized by the ratio β but not its period, influences the adaptation to pulsatile stimuli. When $\tau_0 = 0$, the signal reduces to a step increase in ligand to $\gamma = \gamma_1$, and we recover $\tau_p = \tau_a(\gamma_1)$ from Eq. 14. Similarly, when $\tau_1 = 0$, the signal reduces to the onset of a constant stimulus $\gamma = \gamma_0$, and $\tau_p = \tau_a(\gamma_0)$. Therefore, if $\tau_a(\gamma_1) > \tau_a(\gamma_0)$, τ_p will increase from $\tau_a(\gamma_0)$ to $\tau_a(\gamma_1)$ as β increases from zero to infinity; if $\tau_a(\gamma_1) < \tau_a(\gamma_0)$, τ_p will decrease as β increases.

The influence of the signal amplitude $\delta\gamma = \gamma_1 - \gamma_0$ and of the background level of ligand γ_0 on τ_p is more subtle. What one can say is that, if $k_1 > k_2$ and $k_{-1} > k_{-2}$, τ_p increases as the signal amplitude $\delta\gamma$ or the background ligand level γ_0 increases; on the contrary, the reverse occurs if $k_1 < k_2$ and $k_{-1} < k_{-2}$. In other situations, τ_p changes biphasically when the stimulus amplitude or the background ligand level increases progressively (Fig. 4). On the other hand, an increase in any one of the four parameters $k_i, k_{-i}(i = 1, 2)$ will cause a decrease in the adaptation time τ_p, as shown by Eqs. 12 and 14.

Obviously, a longer adaptation time τ_p means a slower transient process. We may, alternatively, define the rate of adaptation as the rate of decrease in amplitude of $\alpha(t)$ or $D(t)$ during each period, for both the on- and off-phases of the stimulus, as follows:

$$\Delta_j^n \equiv \frac{O_j^n - O_j^{n-1}}{O_j^{n+1} - O_j^n} \qquad (i = 0, 1). \quad (15)$$

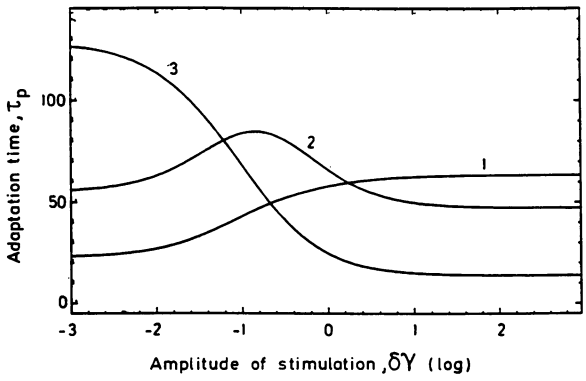

FIGURE 4. The adaptation time τ_p (in min) of the receptor system (Eq. 14) in response to a square-wave, periodic stimulus is drawn as a function of the signal amplitude $\delta\gamma$. The fixed background ligand level is: $\gamma_0 = 0.01$. Other parameters are: $\tau_1 = 6$ min, $\tau_0 = 54$ min, $K_1 = 5$, $K_2 = 0.1$, $c = K_1/K_2 = 50$; moreover, $k_1 = 0.01\ \text{min}^{-1}$, $k_2 = 0.008\ \text{min}^{-1}$ for curve *1*; $k_1 = 0.004\ \text{min}^{-1}$, $k_2 = 0.02\ \text{min}^{-1}$ for curve *2*; and $k_1 = 0.001\ \text{min}^{-1}$, $k_2 = 0.08\ \text{min}^{-1}$ for curve *3*.

A simple calculation shows (see Appendix) that

$$\Delta = \Delta_0^n = \Delta_1^n = e^{\omega_0+\omega_1} > 1 \qquad \text{(for all } n \geq 2\text{)}. \tag{16}$$

What is interesting is that the adaptation rate is always the same during all periods and for both the two phases. By comparison of Eqs. 14 and 16, we obtain Eq. 17:

$$\text{Log}\,(\Delta) = \omega_0 + \omega_1 = \tau_a^{-1}(\gamma_0)\tau_0 + \tau_a^{-1}(\gamma_1)\tau_1 = \frac{T}{\tau_p}. \tag{17}$$

All the above discussions of the adaptation time τ_p can equally apply here to the adaptation rate Δ by just noticing that an increase in the adaptation time corresponds to an exponential decrease in the adaptation rate. The difference is that the former is only influenced by the waveform (characterized by the ratio β) of the stimulus but not by the signal period T for a fixed value of β, while the latter is influenced by both the waveform and the period of the stimulus. From Eq. 17, any increase (decrease) in T, either through an increase (decrease) in τ_0 or τ_1 or both, will cause an exponential increase (decrease) in the adaptation rate.

The above analysis of the transient phase yields four results that are important not only for the process of adaptation in sensory and hormonal systems, but also for the related process of tolerance to drug delivery (Peter et al., 1987): (1) The adaptation time and adaptation rate of the receptor system in response to a pulsatile stimulus are determined not only by the system itself but also by the background ligand level, the amplitude, the period and the waveform of the stimulus. (2) Changes in the parameters governing the receptor desensitization and resensitization, k_i, $k_{-i}(i = 1, 2)$ can markedly alter the tendency of changes in the adaptation time and rate as a function of the ratio between the on-phase and the off-phase of the signal, and the background ligand level. (3) Biphasic changes in the adaptation time (or rate) may occur in response to monotonic changes in stimulus amplitude and background ligand level. (4) The adaptation time is only sensitive to changes in the signal waveform but not to the period of the pulsatile stimulus.

The asymptotic expressions for the fully adapted activity and fraction of desensitized receptor are obtained from Eq. 7, a and b, in the limit $n \to \infty$. Then, the adapted solutions within each phase of the period are given by Eq. 18, a and b:

$$D_j^\infty(t) = D_s(\gamma_j) + (-1)^j Q(\gamma_1, \gamma_0) G_j \exp\left(-\frac{t_j}{\tau_a(\gamma_j)}\right) \tag{18a}$$

$$\alpha_j^\infty(t) = \alpha_s(\gamma_j) - (-1)^j Q(\gamma_1, \gamma_0) P(\gamma_j) G_j \exp\left(-\frac{t_j}{\tau_a(\gamma_j)}\right), \tag{18b}$$

where

$$G_j \equiv \frac{e^{\omega_0+\omega_1} - e^{\omega_j}}{e^{\omega_0+\omega_1} - 1} = \frac{\Delta - e^{\omega_j}}{\Delta - 1} \tag{19}$$

and

$$Q(\gamma_1, \gamma_0) \equiv D_s(\gamma_1) - D_s(\gamma_0). \tag{20}$$

Here $j = 0, 1$ again represents the solution in the off- and on-phases, and time is restricted to the range $0 \leq t_j < \tau_j$ since the solutions are time periodic. These asymptotic solutions allow us to study the long-term influence of the pulsatile signal on the activity of the receptor system.

Dose-response curves for periodic stimuli

Four characteristics of the periodic signal influence the response of the receptor system. Beside the waveform and frequency, which will be considered in Section 3, the background level and the amplitude of the stimulus control the magnitude of the response. This dependence is best displayed in dose-response curves which are the counterpart, for periodic signals, of the dose-response curves established for a single step-increase in stimulus.

To quantify the long-term effect of periodic stimuli, we need some measure based on the activity (implicit here is the assumption, further discussed below, that the cellular response is positively correlated with such measure). For the sake of simplicity, we shall restrict our analysis to the case of exact adaptation for which $\alpha_s(\gamma_j) = \alpha_0$ $(j = 0, 1)$; the exact adaptation conditions selected for illustrative purpose will be those of Eqs. A.5a and A.5b, which relate to the case of a simple receptor conformational change. Then, the basal activity α_0 provides a unique reference value. Although analytical expressions become more complicated, the analysis should yield quantitatively similar results when partial rather than exact adaptation occurs, i.e., when $\alpha_s(\gamma_j)$ differs but remains close to α_0.

As a first approach, we consider the amplitude of the activity, α_{Mj}, defined as the difference between the maximum (minimum) activity at the onset of the on- (off-) phase and the basal activity (represented by the dashed line in Fig. 3), and the integrated activity α_{Tj} for each phase $(j = 0, 1)$. The integrated activity measures the area surrounded by the activity curve and the basal activity line. Similar quantities have been studied by Segel et al. (1986) and Knox et al. (1986) for the case of a step increase in ligand. For the periodic stimulus, these quantities are given, according to Eq. 18, a and b, by Eqs. 21 and 22:

$$\alpha_{Mj} \equiv \alpha_j^\infty(t = 0) - \alpha_0 = (-1)^{1-j} Q(\gamma_1, \gamma_0) P(\gamma_j) G_j \tag{21}$$

$$\begin{aligned}\alpha_{Tj} &\equiv \int_0^{\tau_j} [\alpha_j^\infty(t) - \alpha_0]\, dt = \tau_a(\gamma_j)\alpha_{Mj}(1 - e^{-\omega_j}) \\ &= (-1)^{1-j}\tau_a(\gamma_j) Q(\gamma_1, \gamma_0) P(\gamma_j) \zeta(\omega_0, \omega_1) \\ &= (-1)^{1-j} Q(\gamma_1, \gamma_0) F(\gamma_j) \zeta(\omega_0, \omega_1),\end{aligned} \tag{22}$$

where

$$F(\gamma_j) \equiv \tau_a(\gamma_j)P(\gamma_j) \tag{23}$$

$$\zeta(\omega_1, \omega_0) \equiv \frac{(e^{\omega_0} - 1)(e^{\omega_1} - 1)}{e^{\omega_0+\omega_1} - 1} = 2\frac{\sinh\frac{\omega_0}{2}\sinh\frac{\omega_1}{2}}{\sinh\frac{\omega_0 + \omega_1}{2}}. \tag{24}$$

In these equations, $Q(\gamma_1, \gamma_0)$ represents the difference between the levels of modified receptor at steady state for constant stimuli γ_1 and γ_0 (see Eq. 20); $F(\gamma)$ is the product of the adaptation time by function $P(\gamma)$ which measures the difference between the contributions of the unmodified and modified receptor states to the activity (see Eq. 10).

The two quantities α_M and α_T reflect different aspects of the system's activity after adaptation to the periodic stimulus. The former may be important to processes requiring a high maximum activity level, even of brief duration, above some threshold, while the latter may be useful for processes demanding a long duration of suprathreshold activity. However, they are closely related as shown by Eqs. 21 and 22. The integrated activity α_{Tj} at each phase is the product of the amplitude α_{Mj} by the corresponding adaptation time $\tau_a(\gamma_j)$ and by the factor $(1 - \exp(-\omega_j))$. Particularly, when both phases are very long, i.e., if $\tau_0, \tau_1 \to \infty$, then $G_j = 1$, $\exp(-\omega_j) = 0$, and $\zeta = 1$, so that Eqs. 21 and 22 reduce to the activity amplitude and integrated activity corresponding to a step increase in ligand from γ_0 to γ_1. In that case, the integrated activity α_{Tstep} is just the product of the adaptation time τ_a by the corresponding maximum activity α_{Mstep}.

We shall determine the maximum amplitude and integrated activity only for the on-phase ($j = 1$) in which the activity remains above the basal level, α_0. Such a situation amounts to consider that this basal activity level represents a threshold that must be exceeded for a physiological response to be triggered. This hypothesis ensures that no response is observed in the absence of stimulus, and that a response is triggered during the on-phase of stimulation. Thus, we shall only take into account suprabasal activity levels which, in the case of the square-wave stimulus, only appear during the on-phase of the signal. We rewrite Eqs. 21 and 22, for the on-phase only, as

$$\alpha_M \equiv \alpha_{M1} = \alpha_{Mstep}(\gamma_0, \gamma_1)G_1(\omega_0, \omega_1) \tag{25}$$

$$\alpha_T \equiv \alpha_{T1} = \alpha_{Tstep}(\gamma_0, \gamma_1)\zeta(\omega_0, \omega_1), \tag{26}$$

where

$$\alpha_{Mstep}(\gamma_0, \gamma_1) \equiv Q(\gamma_0, \gamma_1)P(\gamma_1) \tag{27}$$

$$\alpha_{Tstep}(\gamma_0, \gamma_1) \equiv \tau_a(\gamma_1)\alpha_{Mstep}(\gamma_0, \gamma_1) \tag{28}$$

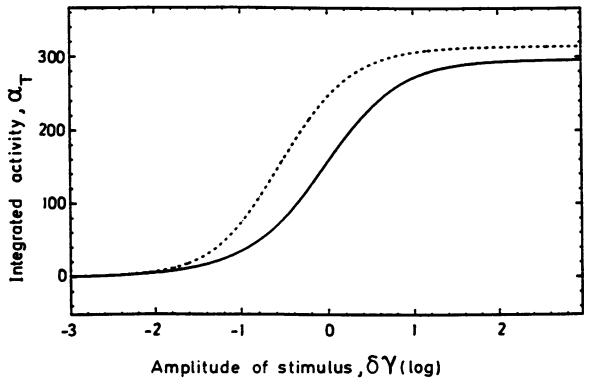

FIGURE 5. Dose-response curve for the adapted integrated activity α_T as a function of the amplitude of the square-wave stimulus. The dotted curve yields the corresponding integrated activity (on a scale eight times larger than that indicated) in response to a step increase in ligand with the same amplitude. The background ligand level is taken as $\gamma_0 = 0.001$. Parameter values are the same as in Fig. 3, with $\tau_1 = 6$ min, $\tau_0 = 54$ min.

are respectively the maximum activity and the integrated activity in response to a corresponding step increase in ligand from γ_0 to γ_1. From Eqs. 25 and 26, we clearly see that the maximum activity and the integrated activity in response to repetitive square-wave stimulation only differ from those in response to a step increase in ligand by the functions G_1 (Eq. 19) and ζ (Eq. 24) which mainly carry the information related to the period and waveform of the signal (see next section).

The influence of the amplitude of the stimulus is shown in Fig. 5 in the form of a dose-response curve obtained at constant background stimulus level and constant period

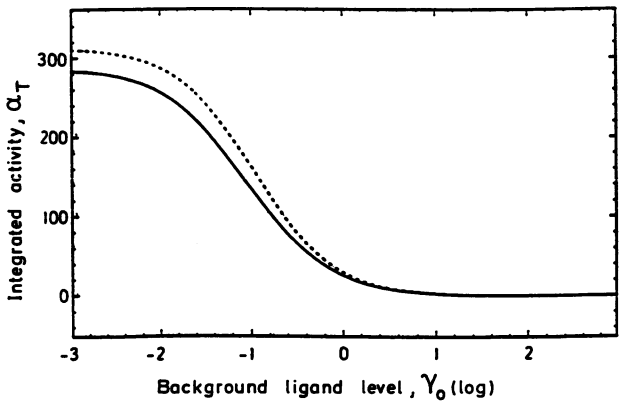

FIGURE 6. Desensitization due to background ligand level. The adapted integrated activity α_T over one period is shown as a function of the level of ligand during the off-phase of stimulation. As in Fig. 5, the dotted curve corresponds to the case of a step increase in ligand, and is drawn with a scale eight times that indicated. The fixed signal amplitude is $\delta\gamma = 20$; other parameter values are as in Fig. 5.

for the integrated activity. The effect of preincubation at various background levels γ_0 on α_T (Eq. 26) in response to a square-wave stimulation of given amplitude and frequency is shown in Fig. 6. The fact that the integrated activity decreases as the background level of ligand rises originates from the progressive desensitization of the receptor induced by the ligand. For comparison, the corresponding curves for a step increase in ligand are drawn as dotted lines in Figs. 5 and 6. These figures show that the dose-response behavior of the receptor system and the influence of prior incubation with ligand are qualitatively the same in the two situations. Similar results are obtained for the maximum activity α_M (Eq. 25).

In both Figs. 5 and 6, the integrated activity for one activity pulse appears to be much smaller for the periodic stimulus than for the single-step increase in ligand. This results from the fact that the integrated activity over a period of the square-wave stimulus depends on the duration of the on-phase which is of 6 min only in the example considered, while for the case of a single step-increase, the integration time is from zero to infinity.

3. Temporal specificity towards periodic stimuli: signal frequency and waveform yielding maximum responsiveness

To determine the influence of the signal frequency and waveform on cellular responsiveness, we now fix the background ligand level and signal amplitude, and focus our attention on the effect of parameters τ_0 and τ_1. In order to guarantee a significant activity, we select from the dose-response curves obtained in Section 2 a pair of values of the background ligand level (γ_0) and of the ligand concentrations during the stimulation (γ_1) that produce a close to maximum activity. Numerical studies indicate that the results do not change significantly when choosing values of γ_1 that produce less than maximum activity.

The activity amplitude α_M and integrated activity α_T have been introduced above as two quantitative measures of the long-term effect of pulsatile stimuli. It is easy to see in Eqs. 25 and 26 that, if γ_1 and γ_0 are fixed, the activity amplitude α_M and the integrated activity α_T are proportional to G_1 and ζ, respectively. One can show by straightforward derivation of Eq. 19 that $\partial G_1/\partial\tau_0 > 0$, $\partial G_1/\partial\tau_1 < 0$. Therefore, we know that the longer (shorter) the off- (on-) phase duration $\tau_0(\tau_1)$, the larger the activity amplitude α_M. On the other hand, an increase in τ_0 or τ_1 will cause an increase in the integrated activity α_T since $\partial\zeta/\partial\tau_j > 0$ ($j = 0, 1$).

If we consider the influence of the signal period $T(=\tau_0 + \tau_1)$ and waveform $\beta(=\tau_1/\tau_0)$, the following result holds for the integrated activity:

$$\frac{\partial\alpha_T}{\partial T} = \frac{\alpha_{Tstep}}{(1+\beta)} \cdot \frac{\tau_a^{-1}(\gamma_0)e^{\omega_0}(e^{\omega_1}-1)^2 + \tau_a^{-1}(\gamma_1)\,\beta e^{\omega_1}(e^{\omega_0}-1)^2}{(e^{\omega_0+\omega_1}-1)^2} > 0 \quad (29a)$$

$$\frac{\partial\alpha_T}{\partial\beta} = \frac{\alpha_{Tstep}T}{(1+\beta)^2} \cdot \frac{\tau_a^{-1}(\gamma_1)e^{\omega_1}(e^{\omega_0}-1)^2 - \tau_a^{-1}(\gamma_0)\,e^{\omega_0}(e^{\omega_1}-1)^2}{(e^{\omega_0+\omega_1}-1)^2}, \quad (29b)$$

where $\omega_0 = \tau_0/\tau_\alpha(\gamma_0) = T/[\tau_a(\gamma_0)(1+\beta)]$, and $\omega_1 = \tau_1/\tau_a(\gamma_1) = T\beta/[\tau_a(\gamma_1)(1+\beta)]$.

Expression 29b indicates that the derivative can vanish, so that α_T passes through an extremum as a function of β. Further differentiation of Eq. 29b for fixed signal period T will show that this extremum is a maximum which corresponds to an optimum waveform β^* determined by

$$\frac{\partial\alpha_T}{\partial\beta} = 0 \Longleftrightarrow \rho_a = \frac{\cosh\omega_0 - 1}{\cosh\omega_1 - 1}, \quad (30)$$

where ρ_a is a constant equal to the ratio of adaptation times $\tau_a(\gamma_1)/\tau_a(\gamma_0)$. The existence of an optimum waveform maximizing the integrated activity is shown in Fig. 7, where α_T is plotted as a function of the ratio $\beta = \tau_1/\tau_0$.

In Fig. 8, the optimum ratio β^* is plotted as a function of the desensitization parameter k_2 (curve *a*) and of the resensitization parameter k_{-1} (curve *b*). These two curves are obtained by solving Eq. 30 for β^* as indicated in Appendix. Curve *a* indicates that larger values of the desensitization constant k_2 correspond to lower values of β^*, while curve *b* shows that β^* rises when the resensitization constant k_{-1} increases; the dependence on k_2 is,

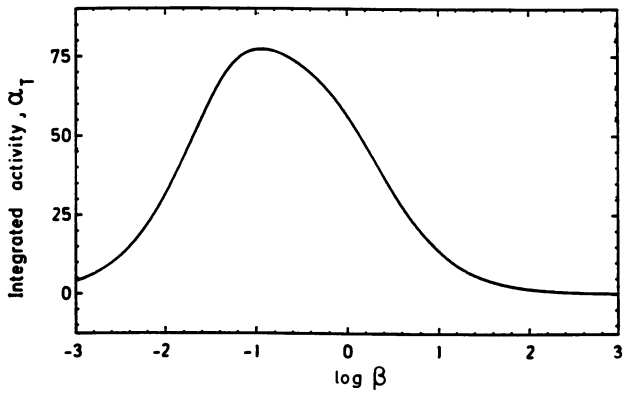

FIGURE 7. Optimal waveform of the square-wave stimulus. The adapted integrated activity α_T is shown as a function of the ratio $\beta = \tau_1/\tau_0$ for a fixed signal period. The curve shows the existence of a particular value of β ($\approx$0.1) which yields maximum integrated activity. The parameter values are: $T = 60$ min, $K_1 = 10$, $K_2 = 0.1$, $c = K_1/K_2 = 100$, $k_1 = 0.00195$ min^{-1}, $k_2 = 0.645$ min^{-1}; $\gamma_0 = 0.001$, $\gamma_1 = 20$; $a_1 = 20$, $a_2 = 101$, $a_3 = 10$, $a_4 = 1$.

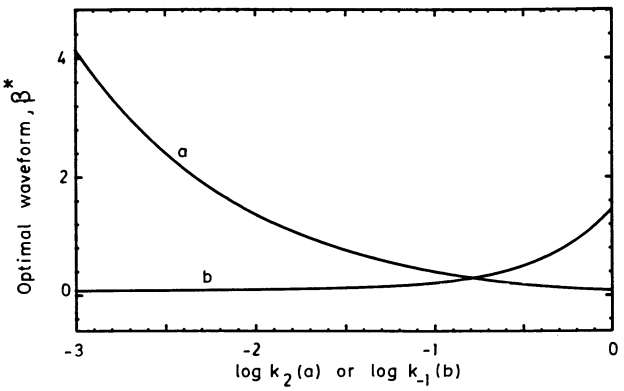

FIGURE 8. The optimum waveform β^* is drawn as a function of the desensitization parameter k_2 (curve *a*), and of resensitization parameter k_{-1} (curve *b*). For curve *a*, $k_{-1} = 0.0195$ min^{-1}; for curve *b*, $k_2 = 0.645$ min^{-1}; other parameter values are the same as in Fig. 7.

however, stronger than that on k_{-1}. These results can readily be explained by noticing the antagonistic effects of k_{-1} and k_2 on β^*: the duration τ_0 of the off-phase required for restoration of full responsiveness decreases as k_{-1} increases, while the duration τ_1 of the on-phase should decrease with increasing k_2 in order to avoid desensitization. Therefore, the optimum ratio $\beta^* = \tau_1^*/\tau_0^*$ should respectively increase or decrease as k_{-1} or k_2 increases.

So far, we have shown that there exists an optimal waveform characterized by a certain ratio τ_1/τ_0 that maximizes the integrated activity over a period. The question arises as to whether there exists a particular value of the period of signaling corresponding to a couple of values for τ_1 and τ_0, that also yields maximum integrated activity. This cannot happen for α_T since Eq. 29a shows that this quantity will always increase when τ_1 and τ_0, i.e., T, rise. In the limit, a single response of maximum amplitude and maximum integrated activity will be elicited when the period of stimulation becomes very large.

From a physiological point of view, however, we may feel that the definition of cellular responsiveness in terms of α_T only is incomplete. Cellular responsiveness should indeed take into account the magnitude of integrated activity (α_T) as well as the number of activity pulses in a given time interval. Therefore, we shall now consider a measure of responsiveness that encompasses these two aspects of the activity changes generated by the periodic stimulus. Such a measure is provided by the dimensionless quantity α_R defined by Eq. 31 as the product of two terms:

$$\alpha_R = \frac{\alpha_T}{\alpha_{Tstep}} \cdot \frac{\alpha_T}{T} = \frac{\tau_a(\gamma_1)\alpha_{Mstep}}{T}\zeta^2, \tag{31}$$

where α_{Mstep} and α_{Tstep} are defined by Eqs. 27 and 28, respectively.

The first term in Eq. 31, related to the magnitude of the integrated activity, is the ratio α_T/α_{Tstep}, which scales the integrated activity during one pulse of the periodic stimulus with respect to the integrated activity corresponding to a step increase in ligand of the same amplitude. The second is the period average of the integrated activity, α_T/T, which takes not only τ_1 but also the off-phase duration τ_0 directly into account; this is easily seen by noticing that in a given time interval $t = nT$, this quantity will yield the total integrated activity $n\alpha_T$ in that time interval.

We shall broadly refer to α_R as cellular responsiveness although we are aware that this quantity provides only a crude, however general, measure not based on an explicit mechanism for coupling the intracellular response to ligand binding.

To determine whether an optimum in cellular responsiveness exists, we differentiate α_R with respect to $\tau_j (j = 0, 1)$ to obtain Eq. 32:

$$\frac{\partial \alpha_R}{\partial \tau_j} = \frac{\alpha_{Tstep}\zeta}{(\tau_0+\tau_1)(e^{\omega_0+\omega_1}-1)} \cdot \left[\frac{2e^{\omega_j}(e^{\omega_{1-j}}-1)^2}{\tau_a(\gamma_j)(e^{\omega_0+\omega_1}-1)} - \frac{(e^{\omega_0}-1)(e^{\omega_1}-1)}{(\tau_0+\tau_1)}\right]. \tag{32}$$

Again in Eq. 32, $\omega_j = \tau_j/\tau_a(\gamma_j)$ $(j = 0, 1)$. Obtaining the second derivative of α_R shows that, for both the on-phase duration τ_1 and the off-phase duration τ_0, there exists an optimum value where the cellular responsiveness is maximum. The optimum value of τ_j is determined by solving Eq. 33

$$\frac{\partial \alpha_R}{\partial \tau_j} = 0 \Longleftrightarrow \frac{2(\tau_0+\tau_1)}{\tau_a(\gamma_j)} = \frac{(e^{\omega_j}-1)(e^{\omega_0+\omega_1}-1)}{(e^{\omega_{1-j}}-1)e^{\omega_j}} \tag{33}$$

for $j = 0$ and 1. If condition 33 is satisfied for $j = 0$ and 1 simultaneously, we obtain the optimal signal pattern (τ_0^*, τ_1^*) which results in maximum cellular responsiveness (see Fig. 9). The existence of this optimum does not depend on the values of γ_0 and γ_1 which determine the amplitude of stimulation. The two conditions expressed by Eq. 33 for $j = 0$ and 1 reduce then to the simpler Eqs. 34a and 34b:

$$\rho_a = \frac{\cosh \omega_0 - 1}{\cosh \omega_1 - 1} \tag{34a}$$

$$1 + 2\left(\frac{\omega_0}{\sqrt{\rho_a}} + \omega_1\sqrt{\rho_a}\right)^2 = \cosh(\omega_0 + \omega_1), \tag{34b}$$

where $\rho_a = \tau_a(\gamma_1)/\tau_a(\gamma_0)$ and $\omega_j = \tau_j/\tau_a(\gamma_j)$ $(j = 0, 1)$. Notice that Eq. 34a is the same as Eq. 30, which specifies the value of β that maximizes the integrated activity α_T.

By solving Eqs. 34a,b as indicated in the Appendix, we obtain the optimum values of τ_0 and τ_1 for the square-wave signal that elicits the highest cellular responsive-

ness. In other words, for given parameter values of the receptor system (k_i, k_{-i}, $i = 1, 2$) and for fixed signal amplitude, Eqs. 34a,b determine both the optimum period $T^*(= \tau_0^* + \tau_1^*)$ and the optimum waveform $\beta^*(= \tau_1^*/\tau_0^*)$ of the stimulation pattern which elicit the "best" response to repetitive stimulation.

In Fig. 9, the cellular responsiveness α_R is plotted as a function of τ_0 and τ_1. The data clearly show the existence of an optimum stimulus pattern predicted by the above analysis. For the particular set of parameter values selected, the solution of Eqs. 34a,b yields $\tau_0^* \approx 53.9$ min, $\tau_1^* \approx 6.1$ min (or $T^* \approx 60$ min, $\beta^* \approx 0.113$). Fig. 9 further indicates that to maintain the cellular responsiveness α_R within 10% from its maximum value, the duration of the on- and off-phase of the stimulus should roughly be kept within the ranges 32.6 min $< \tau_0 <$ 87.4 min for $\tau_1 = \tau_1^*$, and 3.2 min $< \tau_1 <$ 14.6 min for $\tau_0 = \tau_0^*$. The values of τ_0^* and τ_1^* do not change significantly when the signal amplitude $\delta\gamma$ comprises between 1 and 100 or more. When $\delta\gamma$ decreases below unity, for the situation considered in Fig. 9, τ_0^* and τ_1^* progressively rise while the maximum cellular responsiveness α_R diminishes.

In Fig. 10 *a*, the optimal durations of on- (*dashed curve*) and off- (*solid curve*) phases (τ_1^* and τ_0^*) are plotted as functions of the resensitization rate constant k_{-1}. Changes in this parameter mainly induce changes in the optimal off-phase duration τ_0^*, while τ_1^* remains nearly unchanged. In Fig. 10 *b*, the two quantities are plotted as functions of the desensitization rate constant k_2. In contrast to the effect of k_{-1}, changes in k_2 alter the optimal duration of both the on-phase and off-phase, but the variation range of τ_1^* is somehow larger. It appears, therefore, that the specificity towards the duration of the on-phase of the periodic signal is primarily determined by the time scale of receptor desensitization which is characterized by k_2 in the limit $k_2 \gg k_{-2}$. Specificity towards the duration of the off-phase is governed to a certain extent by the time scale of receptor desensitization and, to a larger degree, by the time scale of receptor resensitization which is characterized by k_{-1} under the condition $k_{-1} \gg k_1$.

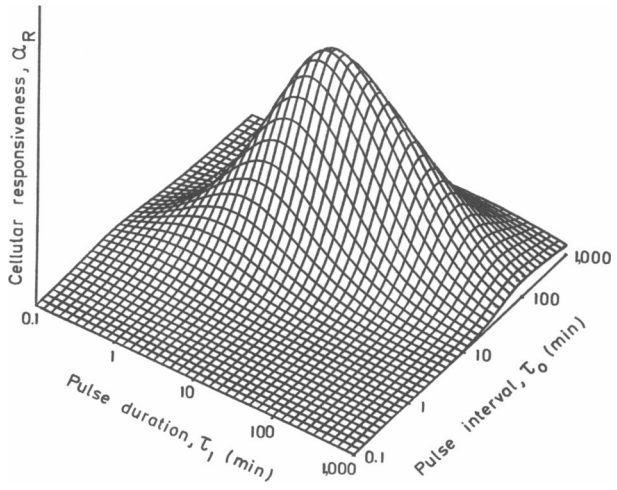

FIGURE 9. Cellular responsiveness α_R as a function of pulse duration τ_1 and pulse interval τ_0. Both τ_1 and τ_0 are drawn in logarithmic scale. At the height of the vertical axis α_R is equal to 1.5. The quantity α_R is obtained according to Eq. 31. Parameter values a_i ($i = 1, 2, 3, 4$) are as in Fig. 3, and k_i, k_{-i} ($i = 1, 2$) are as in Fig. 7.

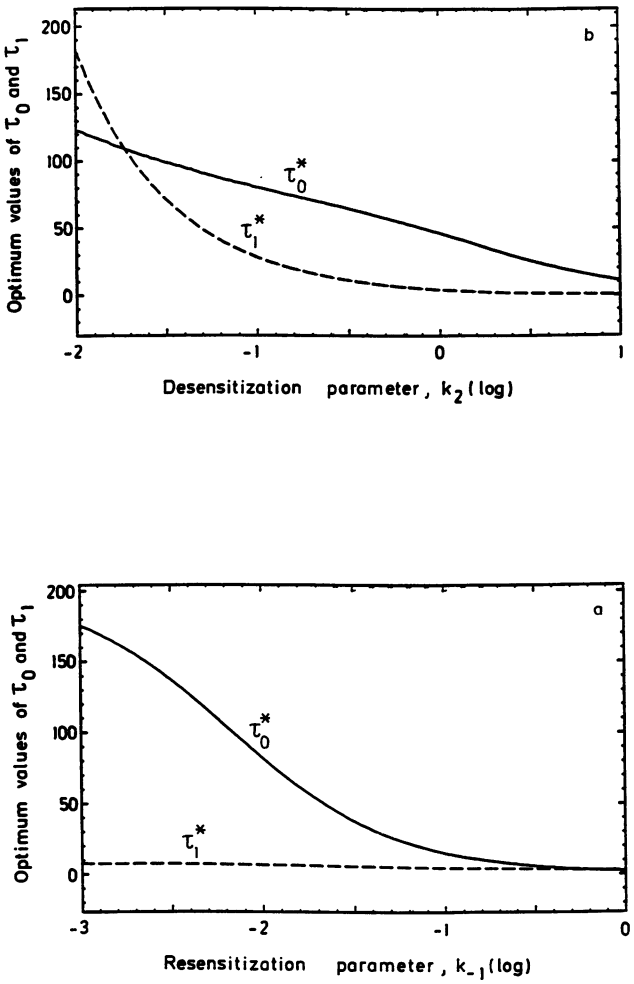

FIGURE 10. The optimum values of τ_1^* (*dashed curves*) and τ_0^* (*solid curves*) are drawn as functions of the resensitization parameter k_{-1} (*a*), and as functions of the desensitization parameter k_2 (*b*). Parameter values are the same as in Fig. 8. The values of τ_1^* and τ_0^* are obtained from Eq. 34a, b as indicated in the Appendix.

4. Extension to more realistic forms of periodic stimuli

All the above results were obtained for the square-wave idealization of the periodic stimulus given by Eq. 6 and

depicted in Fig. 2. In physiological situations, the ligand should decay exponentially, due to a finite half-life, rather than being withdrawn suddenly (as in the square-wave) after it is secreted. Such exponential decay of the stimulus is observed in the experiments in which GnRH pulses are injected in rhesus monkeys (Knobil, 1980).

We therefore consider now the more realistic periodic stimulus defined by Eq. 35 (see also Fig. 11, *bottom panel*):

$$\begin{aligned} \gamma(t) &= \gamma_a && \text{if } t = nT \\ \gamma(t) &= \gamma_a \exp\left(-(t - nT)/\tau_d\right) && \text{if } nT < t < (n+1)T, \end{aligned} \tag{35}$$

where T is the signal period, τ_d is the ligand half-life, γ_a is the signal amplitude, and $n = 0, 1, 2, \ldots$ denotes the successive pulses in the repetitive stimulation. For a given period and amplitude, the duration of stimulation, governed by β for the square-wave stimulus, is governed here by parameter τ_d. The hypothesis of the instantaneous injection implied by Eq. 35 corresponds to some protocols for experiments with GnRH pulses (Badger et al., 1983), and provides an idealization of the situation in which the pulse is given over a brief but finite time (6 min every hour in the experiments of Knobil (1980) with GnRH.

The signal given by Eq. 35 corresponds to the situation where the ligand half-life τ_d is so short compared with the signal period T that almost all ligand molecules are depleted before the next secretion pulse comes. If this is not the case, the level of the ligand at the height of successive pulses will at first increase, because a constant amount γ_a is added at each pulse. We then have to consider the more general stimulus defined by Eq. 36a and b:

$$\gamma(t) = \gamma_M^n \exp\left(-\frac{t - nT}{\tau_d}\right) \tag{36a}$$

$$\gamma_M^n = \sum_{j=0}^{n} \gamma_a \exp\left(-\frac{jT}{\tau_d}\right) = \gamma_a \frac{1 - e^{-n\omega}}{1 - e^{-\omega}}, \tag{36b}$$

where γ_a is the amplitude of ligand secretion, γ_M^n is the maximum level of ligand at the beginning of each pulse; T is the period of the signal, $\omega \equiv T/\tau_d$, $n = 0, 1, 2, \ldots$ represents the successive pulses in the repetitive stimulation, and t is constrained in the range $nT \leq t < (n+1)T$.

After a transient, the stimulus given by Eq 36a,b will reach a steady amplitude. Therefore, there exists an adaptation process in the amplitude of the stimulus itself, characterized by the adaptation time τ_d. For the adapted signal ($n \to \infty$), the maximum and minimum are determined by Eq. 37a and b:

$$\gamma_{max} = \gamma_M^{\infty} = \frac{\gamma_a}{1 - e^{-\omega}} \tag{37a}$$

$$\gamma_{min} = \gamma_{max}\, e^{-\omega} = \frac{\gamma_a e^{-\omega}}{1 - e^{-\omega}} \tag{37b}$$

with

$$\delta\gamma = \gamma_{max} - \gamma_{min} = \gamma_a . \tag{37c}$$

In the limit $\omega = T/\tau_d \to \infty$, the stimulus given by Eq. 36a and b reduces to the stimulus in Eq. 35.

As exemplified by the case of GnRH, for which τ_d and T are of the order of a few minutes and an hour, respectively (Knobil, 1980), the condition $\tau_d \ll T$ is usually satisfied, so that we shall consider the signal given by Eq. 35. A typical activity generated by this kind of stimulus is shown in Fig. 11 (*middle panel*). Also shown (*upper panel*) is the accompanying change in the total fraction of desensitized receptor.

As in the case of square-wave stimulation, we define the activity amplitude α_M as the difference between the

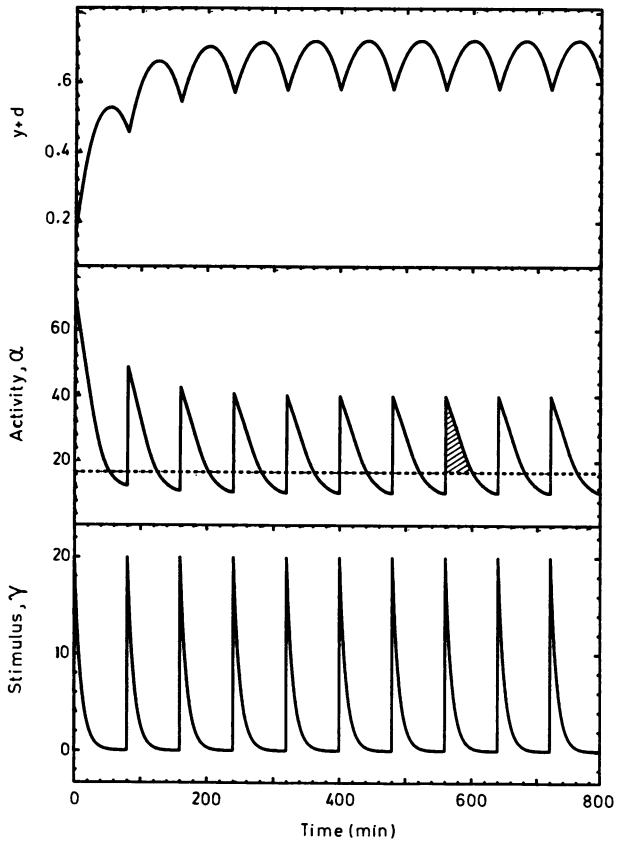

FIGURE 11. Time evolution of the activity (*middle panel*) in response to a periodic signal (Eq. 35) with exponential decay of the ligand (*lower panel*). Also shown is the time evolution of the fraction of desensitized receptor $(Y + D)/R_T$ (*top panel*). The parameters are the same as in Fig. 3, but here $T = 80$ min; moreover, $\gamma_a = 20$ and the half-life of the ligand is taken as $\tau_d = 10$ min. As in Fig. 3, the shaded area represents the integrated activity α_T. The dotted line in the middle panel denotes the basal activity, α_0.

maximum activity and the basal one, and the integrated activity α_T as the area surrounded by the activity curve above the basal activity line after adaptation (shaded area in Fig. 11). We retain the measure α_R, defined by Eq. 31, for cellular responsiveness. No analytical expression can be obtained for α_R in the present situation, so that results reported below were obtained by numerical simulations.

A dose-response curve for the periodic stimulus with exponential decay is plotted in Fig. 12, where the integrated activity α_T is shown as a function of the stimulus amplitude γ_a. As in Fig. 5, the curve extends over a broad stimulus range, but there is a progressive decline in the activity, because of desensitization.

For this more realistic periodic stimulus, an optimum value of the degradation half-life of ligand τ_d exists, that yields a maximum integrated activity (Fig. 13). This shows that an optimum waveform can also be found here, as in the case of square-wave stimulation (compare Fig. 13 with Fig. 7).

In Fig. 14, the cellular responsiveness α_R is plotted as a function of the period of the signal and the half-life of the ligand. Again, as in Fig. 9, the data show the existence of an optimum temporal pattern (T^*, τ_d^*) of the signal that results in maximum responsiveness. For the parameter values chosen in Fig. 9 for the receptor system, this optimum occurs here for $T^* \approx 43.6$ min, $\tau_d^* \approx 3.7$ min. To maintain cellular responsiveness within a deviation of less than 10% from its maximum value, the period of signaling and the half-life for ligand degradation should be kept within the ranges: 30.5 min $< T <$ 75.8 min for $\tau_d = \tau_d^*$, and 2.0 min $< \tau_d <$ 5.1 min for $T = T^*$. These results are in good agreement with those obtained in the analysis of square-wave stimulation, indicating that the square-wave stimulus provides a satisfactory approximation to the more realistic periodic signal. Moreover, the comparison

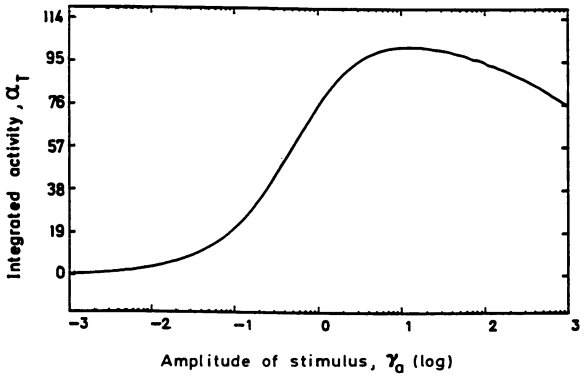

FIGURE 12. Dose-response curve showing the adapted integrated activity α_T as a function of the amplitude of the periodic signal with exponential decay. The parameter values are: $T = 60$ min, $\tau_d = 10$ min, $K_1 = 10$, $K_2 = 0.1$, $c = K_1/K_2 = 100$, $k_1 = 0.003$ min^{-1}, $k_2 = 0.5$ min^{-1}; $a_1 = 20$, $a_2 = 101$, $a_3 = 10$, $a_4 = 1$.

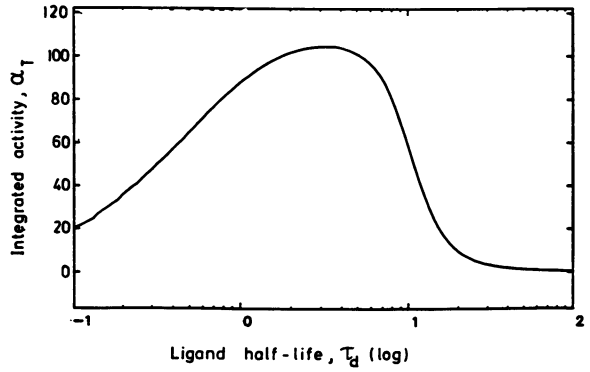

FIGURE 13. Integrated activity α_T in response to the signal with exponential decay as a function of the half-life of the ligand, τ_d. Here also, as in Fig. 7, an optimal pattern of stimulation characterized by an optimum value of τ_d yielding maximum α_T is observed. The parameter values are the same as in Fig. 12, with $\gamma_a = 20$.

of the responses to the two types of signals indicates that the temporal specificity of the periodic stimulus is sharpened when exponential decay of the ligand is taken into account.

5. Application to experimental systems and discussion

Many sensory and hormonal systems have the capability of adapting to constant stimulation. Thus, when the stimulus is increased in a stepwise manner, the target cell displays a transient response as it returns to prestimulus behavior, despite the fact that the level of stimulating

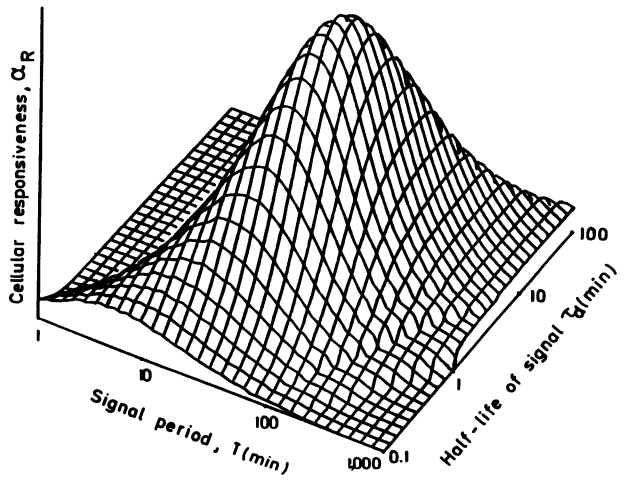

FIGURE 14. Cellular responsiveness α_R (Eq. 31) as a function of the period T and the half-life τ_d of the periodic signal with exponential decay. Both T and τ_d are drawn in logarithmic scale; other parameter values are as in Fig. 9. At the height of the vertical axis α_R is equal to 2.03.

ligand has increased. Models based on receptor desensitization have been proposed to account for such a biphasic response (Macnab and Koshland, 1972; Koshland, 1977; Goldbeter and Koshland, 1982; Segel et al., 1986). Intercellular communication, however, often proceeds in a periodic manner. Here we have shown that cells also adapt to periodic stimuli, and that there exists a pattern of periodic stimulation that maximizes cellular responsiveness. These results suggest that besides the well-recognized conformational specificity associated with the fitting of the ligand to the receptor, there exists a temporal specificity in intercellular communication, associated with pulsatile patterns of stimulation.

To determine the effect of periodic stimulation, we used the general framework of a receptor desensitization model in which the different receptor states with or without ligand generate a certain activity which is ultimately linked to the cellular response (Segel et al., 1986). The nature of the link was not made explicit but will be discussed below. The desensitization considered in the model may take different forms. Thus, it may represent the transition to another conformational state, a process of covalent modification, or a process of down-regulation through receptor internalization.

We showed that a process of adaptation also accompanies periodic stimulation: after a transient phase, the amplitude of the receptor-generated activity indeed settles at a reduced, constant (adapted) value. The rate and magnitude of this adaptation were determined analytically for a square-wave signal, and a dose-response curve was established as a function of such periodic stimulus. This dose-response curve resembles the dose-response curve obtained when the stimulus is given in the form of a single stepwise increase in ligand.

The main result of our study is the demonstration of the existence of a pattern of periodic stimulation that maximizes a quantity α_R taken as a measure of cellular responsiveness. This measure takes into account both the number and the magnitude of activity pulses generated by the periodic signal in a given time interval. For the square-wave stimulus which is characterized by the durations of the on- and off-phases τ_1 and τ_0, we obtained analytically the couple of (τ_0, τ_1) values that maximizes α_R. In other words, there exists a unique value of the stimulation period T, and of the ratio $\beta = \tau_1/\tau_0$ that governs the waveform of the signal, that correspond to an optimum in cellular responsiveness α_R. Similar results were established with the more realistic periodic stimulus in which exponential decay of the ligand is taken into account. An optimum responsiveness is then produced by a couple of particular values of the signal period and half-life of ligand.

To what experimental systems does the present analysis apply? Examples of periodic signaling in intercellular communication range from the periodic generation of cAMP pulses that control aggregation of *Dictyostelium discoideum* amebas to pulsatile patterns of hormone secretion. We shall examine in turn these two phenomena.

Application to cAMP signaling in *Dictyostelium* cells

In *D. discoideum,* the receptor for cAMP is desensitized through reversible phosphorylation (Devreotes and Sherring, 1985). A model based on this process of desensitization has been presented by Martiel and Goldbeter (1987). Besides accounting for autonomous oscillations of cAMP and relay of suprathreshold cAMP pulses, these authors also determined numerically the response of the signaling system to repetitive, square-wave stimulation by extracellular cAMP. Numerical simulations indicated that cAMP synthesis by stimulated cells markedly depends on the interval between successive stimuli.

The present analysis allows one to investigate in a more systematic manner the effect of periodic stimulation by cAMP pulses in *Dictyostelium.* The equations presented here indeed permit to determine the pattern of square-wave stimulation that yields the optimal cellular responsiveness. When taking the experimentally available values for the rate constants governing receptor phosphorylation and dephosphorylation (see last column of Table II in the paper by Martiel and Goldbeter, 1987), we obtain, by the procedure followed to generate Figs. 9 and 10, an optimal square-wave signal for which the on- and off-phases last 3.8 and 5 min, respectively. This result correlates well with the data obtained by Martiel and Goldbeter (1987) in the model for cAMP signaling. In Fig. 15 of their paper, two series of stimuli of 5-min duration were considered, spaced by 5 and 1 min, respectively. The first periodic stimulus produced a nearly maximum response, in contrast to the second stimulus of higher frequency. This is in agreement with the present results, since the 5 min on-, 5 min off-stimulus is very close to the optimum square-wave signal determined in the present model which is closely related to that considered by Martiel and Goldbeter (1987).

In applying our results to cAMP signaling in *Dictyostelium,* we have to remember that under physiological conditions, these cells become excitable prior to aggregation as they amplify suprathreshold cAMP pulses in a pulsatory manner. The effect of periodic stimulation of such excitable cells is likely to differ somewhat from that produced by stimulation of nonexcitable cells. Indeed, whereas the latter only possess a relative refractory period, the former are also characterized by an absolute refractory period (Martiel and Goldbeter, 1987). As a result, the optimum interval between successive stimuli is likely to be larger in the case of excitable cells.

In the experiments of Wurster (1982), however, the amebas did not necessarily acquire yet the excitable response. Therefore our present results provide an explanation for Wurster's findings on the effectiveness of cAMP pulses delivered every 5 min, as compared to that of pulses delivered every 2 min, in promoting cell differentiation. On the other hand, the optimal pattern of repetitive stimulation of nonexcitable cells determined here could be tested experimentally, using the technique of constant stimulation by controlled cAMP signals developed by Devreotes and Steck (1979) for *D. discoideum* cells.

Application to periodic hormonal signaling: the effect of GnRH pulses on pituitary cells

Our results may also apply to the periodic patterns of secretion observed for an increasing number of hormones (Wagner and Filicori, 1987). The episodic release of GnRH with a frequency close to one pulse per hour by the hypothalamus in men and women is the prototype of periodic hormone signaling. The GnRH signal induces the periodic release of the luteinizing hormone (LH) and follicle-stimulating hormone (FSH) by the pituitary. These gonadotropin hormones play an essential role in the control of gonadal development in both males and females, and in the control of ovulation in the latter (Crowley et al., 1985). Although an increasing number of other hormones are found to be secreted periodically into the circulation, the GnRH-induced release of LH and FSH still remains the best-studied example of periodic hormone signaling.

Knobil and co-workers (Belchetz et al., 1978; Knobil, 1980; Wildt et al., 1981; Pohl et al., 1983) have conducted in vivo studies on rhesus monkeys subjected to hypothalamic lesions that suppress the autonomous signal of GnRH. Their experiments showed that continuous addition of GnRH is unable to induce the sustained release of LH and FSH, while a GnRH signal with the physiological frequency of one pulse per hour is capable to produce the normal secretion of gonadotropin hormones. Moreover, periodic GnRH signals with higher or lower frequencies such as two pulses per hour or one pulse per 2 h, also fail to produce the physiological effect. These results led Knobil (1980, 1981) to stress the importance of the temporal pattern of stimulation in the responsiveness of target cells to hormonal stimulation. This factor has now been incorporated into therapeutic programs leading to the restoration of ovulation in previously infertile women suffering from abnormal GnRH secretion (Leyendecker et al., 1980; Reid et al., 1981). Periodic injection of GnRH pulses is also used in males for treatment of a variety of physiological disorders (Santoro et al., 1986; Wagner, 1985). The present results provide a theoretical framework for comprehending these clinical observations on the importance of the temporal pattern of hormone signaling for target cell responsiveness.

Furthermore, McIntosh and McIntosh (1986) have obtained experimental data which are directly relevant to the present analysis. Rather than studying the effect of pulsatile signals of GnRH in vivo, these authors determined the effect of periodic stimuli in perifused sheep pituitary cells. The initial goal of their study was to show that varying the pattern of periodic stimulation by GnRH does not alter the ratio of LH and FSH released by the cells. In that study, square-wave stimuli were used, with varying amplitude and durations of the on- and off-phases. These stimuli are identical to those considered here, which are characterized by the amplitude $\delta\gamma = \gamma_1 - \gamma_0$ and the durations τ_1 and τ_0 of the on- and off-phases, respectively.

The above theoretical predictions compare well with the results of McIntosh and McIntosh (1986) on several counts. First, when determining the effect of the amplitude of the stimulus for a given temporal pattern of stimulation, i.e., at fixed τ_1 and τ_0, they found that the response, as measured by the release of LH and FSH, increases with the GnRH dose but only up to a point, as the response saturates and even slightly decreases when the concentration of GnRH reaches 8.5×10^{-9} M. Dose-response curves published by a number of authors show that the concentration of GnRH yielding half-maximal release of LH and FSH ranges from about 5×10^{-10} (Kéri et al., 1983) to 5×10^{-9} M (Conn et al., 1987). In our study, the dose-response curve of Fig. 5 indicates that the normalized ligand concentration corresponding to half-maximal activity is around $\gamma = 1$. In their experiments, McIntosh and McIntosh (1986) used a maximum ligand level which corresponds to γ values from 1.7 to 17 in our study, depending on the value considered for the midpoint of the dose-response curve. As indicated in Figs. 5 and 12, the integrated activity begins to saturate and even decline when γ rises above 10. We therefore find good agreement with the experimental results and would predict that GnRH levels higher than 8.5×10^{-9} M in the experimental system should induce a further decrease in response, owing to the phenomenon of desensitization.

The second result of the experimental study to which our analysis can directly be related bears on the influence of the durations τ_1 and τ_0 of the GnRH signal on LH and FSH release. McIntosh and McIntosh (1986) considered the values of 2, 5, and 10 min for the stimulus duration τ_1, and the values of 2, 10, 20, 30, 40, 60, and 120 min for the off-phase interval τ_0. For each τ_1, separate experiments were carried out for four of the above values of τ_0, over a total duration of 480 min. The results allow to compare

the effect of τ_0 at a given value of τ_1, and the effect of τ_1 at fixed τ_0 value. The integrated release of LH and FSH always augmented for increasing pulse interval τ_0, at given duration of stimulation τ_1. For a fixed interval between pulses, there was a value of τ_1, among those considered, that produced a larger response. The authors used their data to construct a three-dimensional diagram showing the amount of gonadotropin released per unit of GnRH as a function of both pulse duration (τ_1) and pulse interval (τ_0). Although the diagram contains a limited number of points, it indicates a trend for the existence of an optimal pattern of stimulation. Thus, the largest response is obtained for $\tau_1 = 2$ min and $\tau_0 = 40$ min. When the amount of gonadotropin released is not normalized, the maximum amount secreted occurs for $\tau_1 = 5$ min, $\tau_0 = 60$ min. These values are very close to those obtained in Knobil's experiments in the rhesus monkey (Knobil, 1980), and to the data of Fig. 9 in the present paper. Our result of $\tau_1 = 6$ min, $\tau_0 = 54$ min for the optimal pattern was obtained for a choice of parameter values that was in a certain measure arbitrary; in the absence of experimental values for the parameters characterizing desensitization on a fast time scale, these parameter values were taken so as to yield good agreement with the optimal pattern of GnRH stimulation in vivo, which is one 6-min stimulation every hour (Knobil, 1980; Wildt et al., 1981).

Another set of experimental results to which our analysis can be compared are those obtained by Liu and Jackson (1984) who studied the effect of periodic GnRH pulses on rat anterior pituitary cells in vitro. The experimental curves obtained by these authors with GnRH pulses of varying amplitude and frequency all showed the progressive decline and eventual stabilization of the amplitude of LH release that are demonstrated in Figs. 3 and 11.

In comparing our analysis with the effect of GnRH pulses on gonadotropin release, we rely on the observation that the latter response undergoes desensitization upon prolonged incubation of gonadotropes with GnRH (Adams et al., 1986; Conn et al., 1987). The molecular processes responsible for desensitization have not yet been fully identified. Moreover, it is possible that several processes, possibly characterized by different time courses, contribute to the observed effect. One such process is that of down-regulation, which occurs within 1–3 hours in cell cultures (Conn et al., 1984), but much more slowly in vivo where receptor loss is seen only after 6 h (see, for example, Adams et al., 1986). Desensitization due to depletion of LH and FSH intracellular stores has also been invoked, but desensitization can occur in the absence of gonadotropin release (Jinnah and Conn, 1986) so that it likely involves some uncoupling of the GnRH receptor from the release response. The precise mechanism of this uncoupling is not yet known, but its existence is also supported by other studies (Smith and Vale, 1981; Badger et al., 1983; Adams et al., 1986).

Our analysis suggests that to obtain an optimal stimulus with the characteristics of the GnRH signal observed both in vivo and in vitro, the process of desensitization should be relatively fast, with a half-life of the order of 1–2 min, and the process of resensitization in the absence of ligand should be slower, with a half-life of the order of 30 min. Is there any experimental evidence supporting such fast desensitization process? Experiments with pituitary cells in culture indicate that the release response to a step increase in GnRH immediately rises at the onset of stimulation and shortly thereafter undergoes a biphasic decrease, resulting in a brief peak with a half-life of the order of 1–2 min, and a slower decline with a half-time of the order of hours (Naor et al., 1982; Zilberstein et al., 1983). The fast initial decline in gonadotropin release might result from the depletion of a readily available pool of LH and FSH stored in vesicles close to the cell membrane (Naor et al., 1982). Another possibility, not demonstrated so far, could be that this initial decrease results from some transition of the GnRH receptor into a state uncoupled from the physiological response. Resensitization upon removal of GnRH should bring the receptor back into its active state in less than 1 h. No experimental evidence for a resensitization process characterized by such time course has been obtained. The recovery from refractoriness that follows the removal of a constant GnRH signal has a half-time of 48 h (Adams et al., 1986). This time course, which probably originates from the recovery from down-regulation, is much too slow to account for the efficiency of GnRH pulses delivered with circhoral frequency.

The present results may thus be taken as suggestive of a reversible process of receptor desensitization taking place in minutes for the GnRH-induced transition into the desensitized state, and in close to 1 h for the reverse transition. This process could correspond to a simple conformational change, or to some kind of covalent modification, e.g., reversible phosphorylation. Evidence in favor of such conjecture is provided by a number of sensory or hormonal systems in which desensitization is associated with receptor modification. Thus, adaptation in bacterial chemotaxis is associated with receptor methylation (Koshland, 1979; Springer et al., 1979), whereas receptor phosphorylation appears to underlie adaptation of the cAMP synthesis triggered by ligand binding to the cAMP receptor in *D. discoideum* (Devreotes and Sherring, 1985; Klein et al., 1985) and to the β-adrenergic receptor in turkey erythrocytes (Sibley et al., 1984). Besides providing a link with other sensory and hormonal

systems, this putative desensitization through covalent modification of the GnRH receptor, taking place in minutes, would provide a molecular basis for the optimal induction of gonadotropin release by 6 min-GnRH pulses applied with a circhoral frequency.

The effectiveness of such periodic signal, seen in vivo (Belchetz et al., 1978; Knobil, 1980; Wildt et al., 1981) and in vitro (Smith and Vale, 1981; Liu and Jackson, 1984; McIntosh and McIntosh, 1986; Badger et al., 1983) indeed implies the existence of an adaptation mechanism that is faster than the progressive decline in gonadotrope responsiveness observed in hours upon GnRH stimulation. Additional factors could, however, play a role in desensitization. Thus, some observations point to the existence of a post-receptor desensitization mechanism (Smith et al., 1983). The binding of GnRH to the receptor might trigger, for example, the synthesis of an intracellular inhibitor of the release reaction. The effect of such putative process on the response to periodic stimuli in the present model is currently under investigation. Preliminary results show that an optimal pattern of periodic stimulation is also obtained in these conditions.

Another factor not considered here is the influence of GnRH stimuli on the GnRH receptor concentration. Besides the long-term down-regulation owing to the loss of receptor by internalization, a transient process of up-regulation has been observed. This "priming" effect (Pickering and Fink, 1977) is associated with protein synthesis and may involve the production of new receptor molecules (Clayton, 1982). Such priming by GnRH explains why the second and third responses to GnRH pulses are often larger than the response to the first pulse (McIntosh and McIntosh, 1986). Incorporation of GnRH-induced receptor synthesis and internalization into the model would account for the observed phenomena of up- and down-regulation. These aspects of the response will only modulate the influence of the stimulation pattern, without altering significantly the conclusion of the present study based on a constant receptor level, since down-regulation is a long-term event whereas up-regulation is only transient.

In applying the present results to the effect of cAMP pulses on cAMP secretion in *Dityostelium* and to that of GnRH pulses on gonadotropin release by pituitary cells, the question arises as to the link between the activity generated in the model by ligand binding and the physiological responses. In the case of *Dictyostelium,* activation of adenylate cyclase upon binding of cAMP to the receptor involves a GTP-binding protein (Van Haastert, 1987). The activity coefficients in Eq. 1 provide a global measure of the coupling constants of the liganded and unliganded receptor states with this protein and adenylate cyclase (Segel et al., 1986; Barchilon and Segel, 1988). It would be difficult to carry the analysis of adaptation to periodic stimuli in a model such as that proposed by Martiel and Goldbeter (1987) in which some steps of this activation process are considered in more detail. It is reassuring that the predictions of the present, simple receptor desensitization model as to the optimal pattern of periodic stimulation are in good agreement with the numerical simulations performed on the more detailed model for cAMP signaling based on receptor desensitization.

For gonadotropin release, experiments indicate that binding of GnRH to the receptor on pituitary cells triggers an influx of calcium ions that eventually leads to LH and FSH secretion (Conn et al., 1987). In this system, the activity $A(t)$ would yield a measure of the quantity of calcium entering the cell upon stimulation and, subsequently, of the quantity of gonadotropin released. The activity coefficients could then represent the conductances of the four receptor states which would behave as ion channels.

Besides the GnRH system, the present approach should apply to other hormones which are secreted periodically into the circulation (Wagner and Filicori, 1987). For these hormones too, periodic, pulsatile signaling should represent an optimal mode of intercellular communication (Goldbeter, 1988). The present results show that each periodic signal will be characterized by an optimal pattern yielding maximum responsiveness of target cells. This pattern will be determined by the kinetic properties that underlie desensitization of the receptor specific for the ligand. To the specificity attached to the chemical nature of the ligand, periodic signaling thus adds temporal specificity. The periodic pattern of stimulation introduces new modes of control as it permits to modulate both the magnitude and frequency of the signal in intercellular communication. Such modulation by steroid hormones or neurotransmitters is used in the reproductive system both during the ovarian cycle (Karsch, 1987) and during gonadal maturation leading to puberty (Reiter and Grumbach, 1982).

Frequency specificity is by no means restricted to communication between unicellular organisms such as *Dictyostelium* amebas or between different types of cells within a given organism. In fact, recent observations suggest that frequency encoding might also be used for intracellular signaling based on calcium oscillations triggered by external stimulation (Woods et al., 1987; Berridge et al., 1988). Besides the examples mentioned above and the frequency coding in neural processes, periodic stimuli of appropriate frequency appear to play a significant role in communication by means of pheromones or bioluminescence in insects (Bossert, 1968; Conner, 1985; Conner et al., 1985; Lloyd, 1983). Temporal specificity also extends to periodic auditory stimuli. Thus, the frequency of the courtship song of the male varies in different species of *Drosophila* and serves as a recognition

factor for the female of the corresponding species (Kyriacou and Hall, 1986). It would therefore appear that as far as periodic signaling of specific frequency is concerned, certain cells communicate like male flies sing to females of their species.

APPENDIX

A.1 Steady-state solution and exact adaptation

For a given value of L, the system described by Eq. 2 with the constraint of Eq. 3 always approaches a steady (adapted) state which is determined by:

$$\mathbf{K}(L)\mathbf{C} = 0. \tag{A.1}$$

By solving Eq. A.1, we obtain the following relations:

$$J \equiv k_1 r_s - k_{-1} d_s = k_{-2} y_s - k_2 x_s \tag{A.2a}$$

$$J' \equiv Lk_d d_s - k_{-d} y_s = k_{-r} x_s - Lk_r r_s \tag{A.2b}$$

$$J = J', \tag{A.2c}$$

where the subscript s denotes the concentrations at steady state. Substituting Eq. 3 into these relations, we obtain the steady-state concentrations

$$\begin{aligned} r_s &= (K_1 + \theta k_1^{-1}) d_s \\ x_s &= (\gamma c K_2 - \theta k_2^{-1} - \theta k_{-d}^{-1} K_2) d_s \\ y_s &= (\gamma c - \theta k_{-d}^{-1}) d_s \\ d_s &= \{(1 + K_1) + \gamma c(1 + K_2) \\ &\quad + \theta[k_1^{-1} - k_2^{-1} - k_d^{-1}(1 + K_2)]\}^{-1}, \end{aligned} \tag{A.3}$$

where

$$\theta = \frac{\gamma k_2 (cK_2 - K_1)}{1 + k_2(K_2 k_{-d}^{-1} + k_{-r}^{-1} + \gamma k_1^{-1})} \tag{A.4}$$

and $K_R \equiv k_{-r}/k_r$, $K_D \equiv k_{-d}/k_d$, $K_i \equiv k_{-i}/k_i (i = 1, 2)$, $\gamma \equiv L/K_R$, $c \equiv K_R/K_D$. When detailed balance applies, $c = K_1/K_2$ so that $\theta = 0$, and eq. A.3 takes a much simpler form.

A necessary but not sufficient condition for exact adaptation is (see also Segel et al., 1986):

$$\frac{a_2 - a_3}{a_1 - a_4} = \xi \frac{k_{a2}}{k_{a1}}. \tag{A.5a}$$

To obtain exact adaptation, this condition has to be supplemented by either (Segel et al., 1986)

$$J = 0, \text{ i.e., } K_1 = cK_2 \tag{A.5b}$$

or

$$\xi = 1, \tag{A.5c}$$

where

$$\xi \equiv \frac{\dfrac{a_2 - B}{k_2}}{\dfrac{a_1 - B}{k_1}} = \frac{k_1[(a_2 - a_1)K_1 + a_2 - a_4]}{k_2(a_1 - a_4)}; \tag{A.6}$$

and $B \equiv \alpha_s(\gamma = 0) = (a_1 K_1 + a_4)/(K_1 + 1)$; and $k_{ai} \equiv k_i + k_{-i} (i = 1, 2)$. Condition A.5b is satisfied when the constraint of detailed balance applies to the receptor box; this particular condition does not necessarily hold when the detailed balance condition fails to apply to the rate constants appearing in the receptor box, e.g., in the case of covalent modification (Segel et al., 1986; Waltz and Caplan, 1987). In the latter case, condition A.5c instead of A.5b should supplement condition A.5a to ensure exact adaptation.

A.2 Solution for the case of a step increase in signal

Under the assumption of instantaneous ligand binding, the balance between the liganded and unliganded receptor states is always in equilibrium. Therefore the relations

$$x(t) = \gamma r(t); \quad y(t) = \gamma c d(t) \tag{A.7}$$

always hold. Thus, we have (Segel et al., 1986)

$$y = \frac{\gamma c}{1 + \gamma c} D, \quad d = \frac{1}{1 + \gamma c} D \tag{A.8a}$$

$$x = \frac{\gamma}{1 + \gamma}(1 - D), \quad r = \frac{1}{1 + \gamma}(1 - D), \tag{A.8b}$$

where $D = y + d$; $R = 1 - D = x + r$. Therefore, if we know the value of D, we know all the concentration values from these relations.

The solution for the case of a step increase in ligand from some initial level to γ is:

$$D(t; D_i, \gamma) = D_s(\gamma) + [D_i - D_s(\gamma)] \exp(-t/\tau_a(\gamma)), \tag{A.9}$$

where $D_s(\gamma)$ and $\tau_a(\gamma)$ are defined by Eqs. 8 and 11, D_i is the initial value of D. Substituting Eq. A.9 into the definition of the activity and remembering that $R = 1 - D$, we obtain

$$\begin{aligned} \alpha &= Ra + Db = a - (a - b)D = a - PD \\ &= a - PD_s - P[D_i - D_s] \exp(-t/\tau_a(\gamma)), \end{aligned} \tag{A.10}$$

where a, b, and P are defined by Eqs. 13 and 10. Thus the activity generated by a step increase in ligand is finally given by Eq. A.11:

$$\begin{aligned} \alpha(t; \alpha_i, \gamma) &= \alpha_s(\gamma) - P(\gamma)[D_i - D_s(\gamma)] \\ &\quad \cdot \exp(-t/\tau_a(\gamma)). \end{aligned} \tag{A.11}$$

The steady-state activity $\alpha_s(\gamma)$ is equal to the basal activity $\alpha_s(\gamma = 0)$ if the system obeys the exact adaptation conditions.

A.3 Solution for the case of a square-wave periodic signal

For the square-wave stimulus (6), the solution of system (2) is given by Eq. 7 where the functions O_j^m's, given below, are obtained by recurrence.

For the on-phase:

$$O_1^1 = D_s(\gamma_1) - Q_i e^{-\omega_1}$$
$$O_1^2 = D_s(\gamma_1) - Q(\gamma_1, \gamma_0)\, e^{-\omega_1} + Q(\gamma_1, \gamma_0)\, e^{-(\omega_0+\omega_1)} - Q_i e^{-(\omega_0+\omega_1)-\omega_1}$$

For $n > 2$

$$O_1^n = D_s(\gamma_1) - Q(\gamma_1, \gamma_0)\, e^{-\omega_1} + Q(\gamma_1, \gamma_0)\, e^{-(n-1)(\omega_0+\omega_1)} - Q_i e^{-(n-1)(\omega_0+\omega_1)-\omega_1} + Q(\gamma_1, \gamma_0)(1 - e^{-\omega_1}) \frac{1 - e^{-(n-2)(\omega_0+\omega_1)}}{1 - e^{-(\omega_0+\omega_1)}} e^{-(\omega_0+\omega_1)}. \quad \text{(A.12a)}$$

For the off-phase:

$$O_0^1 = D_s(\gamma_0) + Q(\gamma_1, \gamma_0) e^{-\omega_0} - Q_i e^{-(\omega_0+\omega_1)}$$

For $n \geq 2$

$$O_0^n = D_s(\gamma_0) + Q(\gamma_1, \gamma_0) e^{-\omega_0} - Q_i e^{-n(\omega_0+\omega_1)} - Q(\gamma_1, \gamma_0)(1 - e^{-\omega_0}) \frac{1 - e^{-(n-1)(\omega_0+\omega_1)}}{1 - e^{-(\omega_0+\omega_1)}} e^{-(\omega_0+\omega_1)}, \quad \text{(A.12b)}$$

where $\omega_j \equiv \tau_j/\tau_s(\gamma_j) (j = 0, 1)$; $Q(\gamma_1, \gamma_0) \equiv D_s(\gamma_1) - D_s(\gamma_0)$; $Q_i \equiv D_s(\gamma_1) - D_i$.

We notice that if $\gamma_0 = 0$, $Q_i = Q(\gamma_1, \gamma_0)$; in this case, the above equations take the simpler form:

$$O_1^n = D_s(\gamma_0) + Q(\gamma_1, \gamma_0) G_0 (1 - e^{-n(\omega_0+\omega_1)}) \quad \text{(A.13a)}$$
$$O_0^n = D_s(\gamma_1) - Q(\gamma_1, \gamma_0) G_1 (1 - e^{-n(\omega_0+\omega_1)}) - Q(\gamma_1, \gamma_0) e^{-n(\omega_0+\omega_1)} = - D_s(\gamma_1) - Q(\gamma_1, \gamma_0) G_1 - Q(\gamma_1, \gamma_0) \frac{e^{\omega_1} - 1}{e^{\omega_0+\omega_1} - 1} e^{-n(\omega_0+\omega_1)}; \quad \text{(A.13b)}$$

for $n > 2$, with

$$G_j \equiv \frac{e^{\omega_0+\omega_1} - e^{\omega_j}}{e^{\omega_0+\omega_1} - 1}. \quad \text{(A.13c)}$$

We immediately see that the time needed for the adaptation in the amplitudes of D and α is

$$\tau_p = \frac{T}{\omega_0 + \omega_1} \quad \text{(A.14)}$$

In the limit $n \to \infty$ (or $t \to \infty$), Eqs. A.12 and A.13 reduce to the same asymptotic (adapted) forms:

$$O_1^\infty = D_s(\gamma_0) + Q(\gamma_1, \gamma_0) G_0 \quad \text{(A.15a)}$$
$$O_0^\infty = D_s(\gamma_1) - Q(\gamma_1, \gamma_0) G_1 \quad \text{(A.15b)}$$

Substituting A.15a,b into Eq. 7a,b, we obtain the asymptotic expressions for $D_s^\infty(t)$ and $\alpha_s^\infty(t)$ given by Eq. 18a,b.

To describe the approach to the adapted state, we note, from Eq. 8, that the initial minimum of $D(t)$ is $D_s(\gamma = 0)$, and the first maximum of $\alpha(t)$ is (according to Eq. A.10) $a(\gamma_1) - P(\gamma_1) D_s(\gamma = 0)$. Eq. A.15 indicates that the asymptotic (adapted) minimum of $D(t)$ is O_0^∞, and the corresponding maximum of $\alpha(t)$ is $a(\gamma_1) - P(\gamma_1) O_0^\infty$. Finally Eq. A.14 yields the characteristic time τ_p of this adaptation process. Thus, we obtain the equations describing the progressive decrease in the maximum amplitude of $\alpha(t)$ and the progressive increase in the corresponding minimum amplitude of $D(t)$ (see the dotted curves in Fig. 3):

$$D_{\min}^t = O_0^\infty + [D_s(\gamma = 0) - O_0^\infty] \exp\left(-\frac{t}{\tau_p}\right) \quad \text{(A.16a)}$$
$$\alpha_{\max}^t = a(\gamma_1) - P(\gamma_1) D_{\min}^t \quad \text{(A.16b)}$$

The adaptation rate given by Eq. 16 is obtained from the definition (15) and from Eq. 12 as

$$\Delta_1^n \equiv \frac{O_1^n - O_1^{n-1}}{O_1^{n+1} - O_1^n} = \frac{e^{-(n-2)(\omega_0+\omega_1)} [Q_i(1 - e^{-(\omega_0+\omega_1)}) - Q(\gamma_1, \gamma_0)(1 - e^{-\omega_0})] e^{-\omega_1}}{e^{-(n-1)(\omega_0+\omega_1)} [Q_i(1 - e^{-(\omega_0+\omega_1)}) - Q(\gamma_1, \gamma_0)(1 - e^{-\omega_0})] e^{-\omega_1}} = e^{\omega_0+\omega_1}; \quad \text{(A.17a)}$$

$$\Delta_0^n \equiv \frac{O_0^n - O_0^{n-1}}{O_0^{n+1} - O_0^n} = \frac{e^{-(n-1)(\omega_0+\omega_1)} [Q_i(1 - e^{-(\omega_0+\omega_1)}) - Q(\gamma_1, \gamma_0)(1 - e^{-\omega_0})]}{e^{-(n-1+1)(\omega_0+\omega_1)} [Q_i(1 - e^{-(\omega_0+\omega_1)}) - Q(\gamma_1, \gamma_0)(1 - e^{-\omega_0})]} = e^{\omega_0+\omega_1}. \quad \text{(A.17b)}$$

A.4 Equations yielding the optimal waveform and frequency

The optimal waveform β^* yielding maximum integrated activity is determined by Eq. 30. The latter equation can be cast into the following form:

$$\omega_0 = \ln(f(\omega_1)), \quad \text{(A.18)}$$

where

$$f(\omega_1) \equiv \rho_a(\cosh \omega_1 - 1) + 1 + \sqrt{\rho_a(\cosh \omega_1 - 1)[\rho_a(\cosh \omega_1 - 1) + 2]}. \quad \text{(A.19)}$$

Remembering that $\omega_0 = T/[\tau_s(\gamma_0)(1 + \beta)]$ and $\omega_1 = T\beta/[\tau_s(\gamma_1)(1 + \beta)]$, Eq. A.18 can be transformed into the following one-dimensional iterate map:

$$\beta_{n+1} = \frac{T\tau_a^{-1}(\gamma_0)}{\ln\left(f\left(\frac{T\beta_n}{\tau_a(\gamma_1)(1 + \beta_n)}\right)\right)} - 1. \quad \text{(A.20)}$$

The fixed point of Eq. A.20 obtained by numerical iteration is the solution of Eq. A.18.

The optimal pattern of signaling that elicits maximum cellular responsiveness is determined by Eq. 34. Noticing that Eq. 34a is identical to Eq. 30, it can therefore be transformed into Eq. A.18. Substituting Eq. A.18 into Eq. 34b, we obtain

$$g(\omega_1) = h(\omega_1), \quad \text{(A.21)}$$

where:

$$g(\omega_1) \equiv 1 + 2\left(\frac{\ln(f(\omega_1))}{\sqrt{\rho_a}} + \omega_1\sqrt{\rho_a}\right)^2; \qquad \text{(A.22a)}$$

$$h(\omega_1) \equiv \cosh(\ln(f(\omega_1)) + \omega_1). \qquad \text{(A.22b)}$$

Solving Eq. A.21 numerically by finding the ω_1 value for which the equality of the two sides holds, we obtain ω_1^*. Substituting that value into Eq. A.18, yields ω_0^*, and, finally, (τ_0^*, τ_1^*) or (T^*, β^*).

This work was supported by the Instituts Internationaux de Physique et de Chimie Fondés par E. Solvay, and by the Belgian National Incentive Program on Fundamental Research in Life Sciences launched by the Science Policy Programming Services of the Prime Minister's Office (SPPS).

Received for publication 13 April 1988 and in final form 7 July 1988.

REFERENCES

Adams, T. E., S. Cumming, and B. M. Adams. 1986. Gonadotropin-releasing hormone (GnRH) receptor dynamics and gonadotrope responsiveness during and after continuous GnRH stimulation. *Biol. Reprod.* 35:881-889.

Avgerinos, P. C., T. H. Schurmeyer, P. W. Gold, T. P. Tomai, D. L. Loriaux, R. J. Sherins, G. B. Cutler, Jr., and G. P. Chrousos. 1986. Pulsatile administration of human corticotropin-releasing hormone in patients with secondary adrenal insufficiency: restoration of the normal cortisol secretory pattern. *J. Clin. Endocrinol. Metab.* 62:816–821.

Badger, M. T., J. S. Loughlin, and P. G. Naddaff. 1983. The luteinizing hormone-releasing hormone (LHRH)-desensitized rat pituitary: luteinizing hormone responsiveness to LHRH in vitro. *Endocrinology.* 112:793–799.

Barchilon, M., and L. A. Segel. 1988. Adaptation, oscillations and relay in a model for cAMP secretion in cellular slime molds. *J. Theor. Biol.* In press.

Bassett, N. S., and P. D. Gluckman. 1986. Pulsatile growth hormone secretion in the ovine fetus and neonatal lamb. *J. Endocrinol.* 109:307–312.

Belchetz, P. E., T. M. Plant, Y. Nakai, E. J. Keogh and E. Knobil. 1978. Hypophysial responses to continuous and intermittent delivery of hypothalamic gonadotropin-releasing hormone. *Science (Wash. DC).* 202:631–633.

Berridge, M., P. H. Cobbold, and K. S. R. Cuthbertson. 1988. Spatial and temporal aspects of cell signalling. *Philos. Trans. R. Soc. Lond. B. Biol. Sci.* In press.

Borges, J. L. C., R. M. Blizzard, W. S. Evans, R. Furlanetto, A. D. Rogol, D. L. Kaiser, J. Rivier, W. Vale, and M. O. Thorner. 1984. Stimulation of growth hormone (GH) and somatomedin C in idiopathic GH-deficient subjects by intermittent pulsatile administration of synthetic human pancreatic tumor GH-releasing factor. *J. Clin. Endocrinol. Metab.* 59:1–6.

Bossert, W. H. 1968. Temporal patterning in olfactory communication. *J. Theor. Biol.* 18:157–170.

Brabant, G., A. Brabant, U. Ranft, K. Ocran, J. Köhrle, R. D. Hesch, and A. von zur Mühlen. 1987. Circadian and pulsatile thyrotropin secretion in euthyroid man under the influence of thyroid hormone and glucocorticoid administration. *J. Clin. Endocrinol. Metab.* 65:83–88.

Cazalis, M., G. Dayanithi, and J. J. Nordmann. 1985. The role of patterned burst and interburst interval on the excitation-coupling mechanism in the isolated rat neural lobe. *J. Physiol. (Lond.).* 369:45–60.

Cesari, L. 1971. Asymptotic Behavior and Stability Problems in Ordinary Differential Equations. Springer-Verlag, Berlin. 271 pp.

Clayton, R. N. 1982. Gonadotropin-releasing hormone modulation of its own pituitary receptors: evidence for biphasic regulation. *Endocrinology.* 111:152–161.

Conn, P. M., C. A. McArdle, W. V. Andrews, and W. R. Huckle. 1987. The molecular basis of gonadotropin-releasing hormone (GnRH) action in the pituitary gonadotrope. *Biol. Reprod.* 36:17–35.

Conn, P. M., D. C. Rogers, and S. G. Seay. 1984. Biphasic regulation of the gonadotropin-releasing hormone receptor by receptor microaggregation and intracellular Ca^{2+} levels. *Mol. Pharmacol.* 25:51–55.

Conn, P. M., D. Staley, C. Harris, W. V. Andrews, W. C. Gorospe, C. A. McArdle, W. R. Huckle, and J. Hanson. 1986. Mechanism of action of gonadotropin releasing hormone. *Annu. Rev. Physiol.* 48:495–513.

Conner, W. E. 1985. Temporally patterned chemical communication: is it feasible? *In* Perspectives in Ethology. Vol. 6. Mechanisms. P. P. G. Bateson and P. H. Klopfer, editors. Plenum Press, New York. 287–301.

Conner, W. E., R. P. Webster, and H. Itagaki. 1985. Calling behavior in arctiid moths: the effects of temperature and wind speed on the rhythmic exposure of the sex attractant gland. *J. Insect Physiol.* 31:815–820.

Crowley, W. F., Jr., M. Filicori, D. I. Spratt, and N. F. Santoro. 1985. The physiology of gonadotropin-releasing hormone (GnRH) secretion in men and women. *Rec. Prog. Horm. Res.* 41:473–531.

Devreotes, P. N., and T. L. Steck. 1979. Cyclic 3',5' AMP relay in *Dictyostelim discoideum.* II. Requirements for the initiation and termination of the response. *J. Cell Biol.* 80:300–309.

Devreotes, P. N., and J. A. Sherring. 1985. Kinetics and concentration dependence of reversible cAMP-induced modification of the surface cAMP receptor in *Dictyostelium. J. Biol. Chem.* 260:6378–6384.

Eggena, P. 1987. Hydroosmotic responses to short pulses of vasotocin by toad bladder. *Am. J. Physiol.* 252:E705–E711.

Goldbeter, A. 1987. Periodic signaling and receptor desensitization: from cAMP oscillations in *Dictyostelium* cells to pulsatile patterns of hormone secretion. *In* Temporal Disorder in Human Oscillatory Systems. L. Rensing, U. an der Heiden, and M. C. Mackey, editors. Springer-Verlag, Berlin. 15–23.

Goldbeter, A. 1988. Periodic signaling as an optimal mode of intercellular communication. *News Physiol. Sci.* 3:103–105.

Goldbeter, A., and D. E. Koshland, Jr. 1982. Simple molecular model for sensing and adaptation based on receptor modification with application to bacterial chemotaxis. *J. Mol. Biol.* 161:395–416.

Hsia, J. A., E. L. Hewlett, and J. Moss. 1985. Heterologous desensitization of adenylate cyclase with prostaglandin E_1 alters sensitivity to inhibitory as well as stimulatory agonists. *J. Biol. Chem.* 260:4922–4926.

Jinnah, H. A., and P. M. Conn. 1986. Gonadotropin-releasing hormone-mediated desensitization of cultured rat anterior pituitary cells can be uncoupled from luteinizing hormone release. *Endocrinology.* 118:2599–2604.

Karsch, F. J. 1987. Central actions of ovarian steroids in the feedback

regulation of pulsatile secretion of luteinizing hormone. *Annu. Rev. Physiol.* 49:365–382.

Katz, F. H., J. A. Smith, J. P. Lock, and D. E. Loeffel. 1979. Plasma vasopressin variation and renin activity in normal active humans. *Horm. Res.* 10:289–302.

Kéri, G., K. Nikolics, I. Teplan, and J. Molnar. 1983. Desensitization of luteinizing hormone release in cultured pituitary cells by gonadotropin-releasing hormone. *Mol. Cell. Endocrinol.* 30:109–120.

Klein, P., A. Theibert, D. Fontana, and P. N. Devreotes. 1985. Identification and cyclic-AMP induced modification of the cyclic AMP receptor in *Dictyostelium discoideum*. *J. Biol. Chem.* 260:1757–1764.

Knobil, E. 1980. The neuroendocrine control of the menstrual cycle. *Rec. Prog. Horm. Res.* 36:53–88.

Knobil, E. 1981. Patterns of hormonal signals and hormone action. *N. Engl. J. Med.* 305:1582–1583.

Knox, B. E., P. N. Devreotes, A. Goldbeter, and L. A. Segel. 1986. A molecular mechanism for sensory adaptation based on ligand-induced receptor modification. *Proc. Natl. Acad. Sci. USA.* 83:2345–2349.

Komjati, M., P. Bratusch-Marrain, and W. Waldhausl. 1986. Superior efficacy of pulsatile versus continuous hormone exposure on hepatic glucose production in vitro. *Endocrinology.* 118:312–319.

Koshland, D. E., Jr., 1977. A response regulator model in a simple sensory system. *Science (Wash. DC).* 196:1055–1063.

Koshland, D. E., Jr. 1979. A model regulatory system: bacterial chemotaxis. *Physiol. Rev.* 59:811–862.

Kyriacou, C. P., and J. C. Hall. 1986. Interspecific genetic control of courtship song production and reception in *Drosophila*. *Science (Wash. DC).* 232:494–497.

Leyendecker, G., L. Wildt, and M. Hansmann. 1980. Pregnancies following chronic intermittent (pulsatile) administration of GnRH by means of a portable pump ("Zyklomat"): a new approach to the treatment of infertility in hypothalamic amenorrhea. *J. Clin. Endocrinol. Metab.* 51:1214–1216.

Liu, T. C., and G. L. Jackson. 1984. Long term superfusion of rat anterior pituitary cells: Effects of repeated pulses of gonadotropin-releasing hormone at different doses, durations and frequencies. *Endocrinology.* 115:605–613.

Lloyd, J. E. 1983. Bioluminescence and communication in insects. *Annu. Rev. Entomol.* 28:131–160.

Macnab, R. M., and D. E. Koshland, Jr. 1972. The gradient sensory mechanism in bacterial chemotaxis. *Proc. Natl. Acad. Sci. USA.* 69:2509–2512.

Martiel, J.-L., and A. Goldbeter. 1987. A model based on receptor desensitization for cyclic AMP signaling in *Dictyostelium* cells. *Biophys. J.* 52:807–828.

Matthews, D. R., B. A. Naylor, R. G. Jones, G. M. Ward, and R. C. Turner. 1983. Pulsatile insulin has greater hypoglycemic effect than continuous delivery. *Diabetes.* 32:617–621.

McIntosh, J. E. A., and R. P. McIntosh. 1986. Varying the patterns and concentrations of gonadotropin-releasing hormone stimulation does not alter the ratio of LH and FSH release from perifused sheep pituitary cells. *J. Endocrinol.* 109:155–161.

Monod, J. 1978. The phenomenon of enzymatic adaptation, and its bearings on problems of genetics and cellular differentiation. *In* Selected Papers in Molecular Biology. A. Lwoff and A. Ullmann, editors. Academic Press, Inc., New York. 68–134.

Naor, Z., M. Katikineni, E. Loumaye, A. G. Vela, M. L. Dufau, and K. J. Catt. 1982. Compartmentalization of luteinizing hormone pools: dynamics of gonadotropin releasing hormone action in superfused pituitary cells. *Mol. Cell Endocrinol.* 27:213–220.

Peter, A., C. A. Grimbergen, J. W. Kraal, and J. H. Engelbart. 1987. An approach to the modeling of the tolerance mechanism in the drug effect. I. The drug effect as a disturbance of regulations. *J. Theor. Biol.* 127:413–426.

Pickering, A. J. M. C., and G. Fink. 1977. A priming effect of luteinizing hormone releasing factor with respect to release of follicle-stimulating hormone in vitro and in vivo. *J. Endocrinol.* 75:155–159.

Pohl, C. R., D. W. Richardson, J. S. Hutchison, J. A. Germak, and E. Knobil. 1983. Hypophysiotropic signal frequency and the functioning of the pituitary-ovarian system in the rhesus monkey. *Endocrinology.* 112:2076–2080.

Redekopp, C., C. H. G. Irvine, R. A. Donald, J. H. Livesey, W. Sadler, M. G. Nicholls, S. L. Alexander, and M. J. Evans. 1986. Spontaneous and stimulated adrenocorticotropin and vasopressin pulsatile secretion in the pituitary venous effluent of the horse. *Endocrinology.* 118:1410–1416.

Reid, R. L., G. R. Leopold, and S. S. C. Yen. 1981. Induction of ovulation and pregnancy with pulsatile luteinizing hormone-releasing factor: dosage and mode of delivery. *Fertil. Steril.* 36:553–559.

Reiter, E. O., and M. M. Grumbach. 1982. Neuroendocrine control mechanisms and the onset of puberty. *Annu. Rev. Physiol.* 44:595–613.

Santoro, N., M. Filicori, and W. F. Crowley, Jr. 1986. Hypogonadotropic disorders in men and women: diagnosis and therapy with pulsatile gonadotropin-releasing hormone. *Endocr. Rev.* 7:11–23.

Segel, L. A., A. Goldbeter, P. N. Devreotes, and B. E. Knox. 1986. A mechanism for exact sensory adaptation based on receptor modification. *J. Theor. Biol.* 120:151–179.

Sibley, D. R., J. R. Peters, P. Nambi, M. G. Caron, and R. J. Lefkowitz. 1984. Desensitization of turkey erythrocyte adenylate cyclase. β-adrenergic receptor phosphorylation is correlated with attenuation of adenylate cyclase activity. *J. Biol. Chem.* 259:9742–9749.

Smith, M. A., M. H. Perrin, and W. W. Vale. 1983. Desensitization of cultured pituitary cells to gonadotropin-releasing hormone: evidence for a post-receptor mechanism. *Mol. Cell. Endocrinol.* 30:85–96.

Smith, M. A., and W. W. Vale. 1981. Desensitization to gonadotropin-releasing hormone observed in superfused pituitary cells on cytodex beads. *Endocrinology.* 108:752–759.

Springer, M. S., M. F. Goy, and J. Adler. 1979. Protein methylation in behavioral control mechanisms and in signal transduction. *Nature (Lond.).* 280:279–284.

Van Haastert, P. J. M. 1987. Alteration of receptor/G-protein interaction by putative protein kinase activity in *Dictyostelium discoideum* membranes. *J. Biol. Chem.* 262:3239–3243.

Verdin, E., M. Castillo, A. S. Luyckx, and P. J. Lefebvre. 1984. Similar metabolic effects of pulsatile versus continuous human insulin delivery during euglycemic, hyperinsulinemic glucose clamp in normal man. *Diabetes.* 33:1169–1174.

Wagner, T. O. F., editor. 1985. Pulsatile LHRH Therapy of the Male. TM-Verlag, Hameln, Federal Republic of Germany. 148 pp.

Wagner, T. O. F., and M. Filicori, editors. 1987. Episodic Hormone Secretion: From Basic Science to Clinical Application. TM-Verlag, Hameln, Federal Republic of Germany. 260 pp.

Waltz, D., and S. R. Caplan. 1987. Consequence of detailed balance in a model for sensory adaptation based on ligand-induced receptor modification. *Proc. Natl. Acad. Sci. USA.* 84:6152–6156.

Weiss, P. 1947. The problem of specificity in growth and development. *Yale J. Exp. Biol. Med.* 19:235–278.

Weizmann, R. E., D. A. Fisher, J. J. DiStefano III, and C. M. Bennett. 1977. Episodic secretion of arginine vasopressin. *Am. J. Physiol.* 233:E32–E36.

Wildt, L., A. Hausler, G. Marshall, J. S. Hutchison, T. M. Plant, P. E. Belchetz, and E. Knobil. 1981. Frequency and amplitude of gonadotropin releasing hormone stimulation and gonadotropin secretion in the rhesus monkey. *Endocrinology.* 109:376–385.

Woods, N. M., K. S. R. Cuthbertson, and P. H. Cobbold. 1987. Agonist-induced oscillations in cytoplasmic free calcium concentration in single rat hepatocytes. *Cell Calcium.* 8:79–100.

Wurster, B. 1982. On induction of cell differentiation by cyclic AMP pulses in *Dictyostelium discoideum. Biophys. Struct. Mech.* 9:137–143.

Zilberstein, M., H. Zakut, and Z. Naor. 1983. Coincidence of down-regulation and desensitization in pituitary gonadotrophs stimulated by gonadotropin-releasing hormone. *Life Sci.* 32:663–669.